

## CHAPTER 3

### Results and Discussions

#### Part I Plant extraction

##### **Plant preparation**

From the literature reviews and folklore medicine recipe, it was found that there are many plants involved inhibiting activity of aromatase including for healing breast cancer and/or ovarian cancer, or claimed as testosterone booster plants were used in Thailand. Therefore, the 22-selected Thai plants were indicated as Table 3.1.

##### **Plant maceration and fractionation**

After maceration these plants with ethanol, the color of extracts can be divided into 3 groups; dark brown or black extracts were obtained from leaf, the dark yellow extract was obtained from bark of *O. indicum*, and the light yellow extract was obtained from *D. lablab*. The weight of ethanolic extracts were in range 0.6-3.2 g obtained from 20 g of plant powder. Interestingly, the fractions of *O. indicum* revealed in yellow color. Especially, the ethyl acetate extract provided light yellow as the color of flavone (Swain, 1976). The weight of ethyl acetate extracts were in range 1.8-2.2 g were obtained from 20 g of plant powder. The different color of extract and yield obtained should be also influenced by part of plant, harvest period and plant age.

Table 3.1 The selected 22-Thai plants for screening aromatase inhibitory activity

Scientific name	Thai name	Part
<i>Ageratum conyzoides</i> L.	Sab-Rang-Sab-Ga	leave
<i>Allium cepa</i> var. <i>aggregatum</i>	Hom	leave
<i>Artabotrys siamensis</i> Miq.	Ga-Ra-Weg	leave
<i>Cananga odorata</i> (Lamk.) Hook.f. et Th.	Ga-Dung-Nga	leave
<i>Catharanthus roseus</i> (L.) G. Don.	Paeng-Pouy-Farang	leave
<i>Cleistocalyx nervosum</i> var. <i>paniala</i>	Ma-Kiang	leave
<i>Coriandrum sativum</i> L.	Pak-She	leave
<i>Cycas revoluta</i> Thunb.	Pong-Ye-Pun	leave
<i>Dolichos lablab</i> L.	Tour-Pap	legume
<i>Millingtonia hortensis</i> L.f.	Peep	leave
<i>Mimusops elengi</i> L.	Pi-Kul	leave
<i>Momordica charantia</i> L.	Ma-Ra-Khee-Nok	leave
<i>Moringa oleifera</i> Lam.	Ma-Room	leave
<i>Nymphaea nouchali</i> Burm. f.	Bour	leave
<i>Oroxylum indicum</i> (L.) Kurz	Pae-Gar	bark
<i>Passiflora edulis</i> Sims	Sow-Wa-Rose	leave
<i>Passiflora foetida</i> L.	Kra-Tok-Rok	leave
<i>Plantago major</i> L.	Pak-Gad-Num	leave
<i>Punica granatum</i> L.	Tub-Tim	leave
<i>Spondias pinnata</i> (L. f.) Kurz	Ma-Kok	leave
<i>Terminalia catappa</i> L.	Hu-Kwang	leave
<i>Wrightia religiosa</i> Benth	Moke	leave

## **Part II Screening of aromatase inhibitory activity from 22 Thai plants**

### **Microsome preparation**

Microsome is the fraction of the endoplasmic reticulum (ER) when eukaryotic cell was broken-up. Normally, microsome is not found in healthy living cell. It can be separated from other cellular debris by differential ultracentrifugation. The unbreakable cell, nucleus, and mitochondria is sediment out at 10,000 x g, whereas soluble enzymes and fragmented ER, containing cytochrome P450, remain in supernatant. After using high ultracentrifuge at 105,000 x g, microsome is sediment out as pellet but the soluble enzymes still remain in the supernatant. In fish, microsome has a reddish color (Figure 3.1) due to the presence of heme as indicated by Richards (2014).

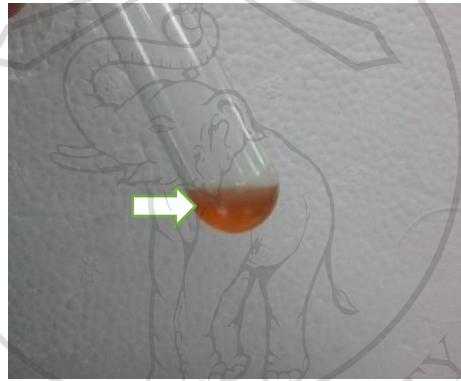


Figure 3.1 The reddish microsome was obtained from healthy tilapia

Microsome from the liver of animal consists of Cytochrom P450 enzymes for drug and steroid hormone metabolism. There are many report indicated that the activity of some enzyme in male microsome are different from female due to difference in sex-related rate of metabolism (Wang, 2002; Shaya, 2014). To examine the effect of AIs on enzyme activity, microsome from male and female tilapia were investigated. The SDS-PAGE patterns of microsome were shown in Figure 3.2.

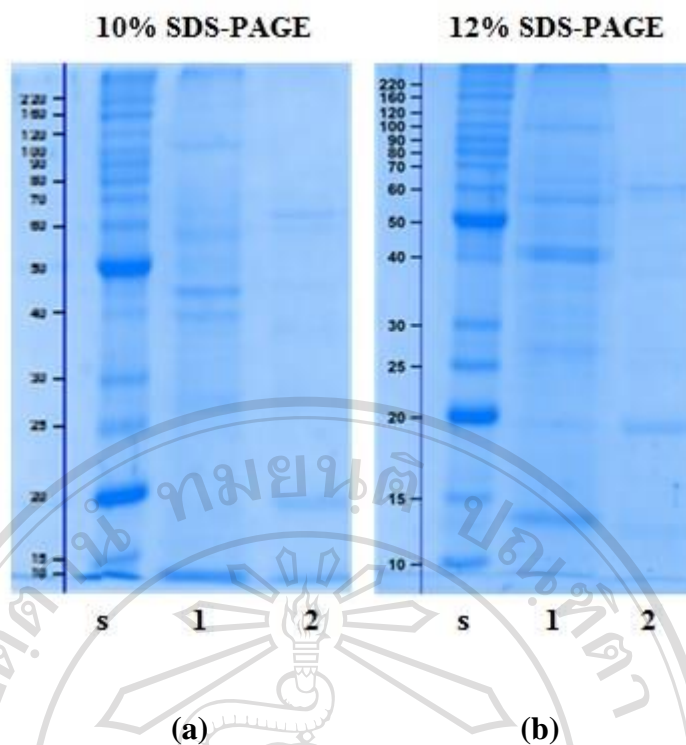


Figure 3.2 SDS gel electrophoresis patterns of microsomes prepared in male (a) and female (b) were obtained on 10% and 12% acrylamide gel, respectively.

SDS-PAGE was used to analyze microsome fractions revealing seven prominent bands in male microsome (lane 1) and two prominent bands in female microsome (lane 2). Comparing the electrophoretic mobility of microsome fractions with standard protein, the major band protein were estimate by Gel Doc™ EZ Imager (Bio-Rad Laboratories, Inc., Australia) reveal major band of male microsome at 13.3, 20.9, 29.8, 44.4, 50.7, 58.5 and 110.5 kDa and female microsome at 19.3 and 67.2 kDa. The different sizes of microsome in male and female tilapia microsome maybe came from the different shape and morphology of endoplasmic reticulum (ER) fractions, and rough/smooth ER content (Lavoie, 2008). Thus, the microsome was examined under scanning electron microscope (SEM). The results of SEM examination was revealed in Figure 3.3.

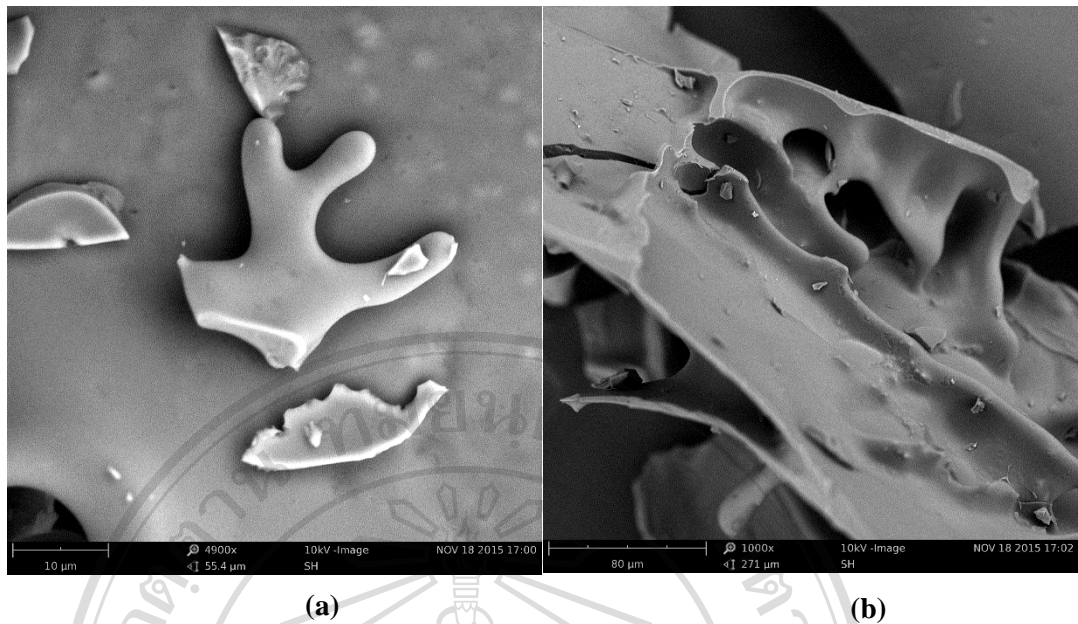


Figure 3.3 SEM micrographies of microsomes at 4900 x (a) and 1000 x (b), respectively

It was found that the morphology of lyophilized microsomal fractions revealed different sizes in ranged ten to more than hundred micrometer resulted the visual protein bands were observed in various molecular weight on SDS-PAGE gel. Interestingly, it was found that the yield of the obtained fish microsomes was influenced by the age and body weight of the fish as shown in Table 3.2. The results suggest that higher yield of fish microsomes should be extracted from the adult fish with higher body weight.

The results in Table 3.1 revealed that yield of microsomes was also resulted from the age and body weight of fish which possible exposure to various exogenous compounds activated smooth/rough ER production during fish culturing (Akdogan, 2010). The furthermore study on microsomal enzyme activity of both sexes was also done in both freshly prepared and lyophilized forms. It was found that the activities of microsome from both male and female tilapia have similar in pattern of enzyme response (Figure 3.4).

Table 3.2 The effects of age and body weight of Nile tilapia on the yield of microsomes  
(n = 3; Mean  $\pm$  SD).

Body weight (g)	Age (month)	Extracted microsomes (mg)
150-160	3-4	0 $\pm$ 0
170-180	3-4	0 $\pm$ 0
190-200	3-4	0 $\pm$ 0
220-230	5-6	27 $\pm$ 6
240-250	5-6	41 $\pm$ 16
300-320	5-6	198 $\pm$ 33

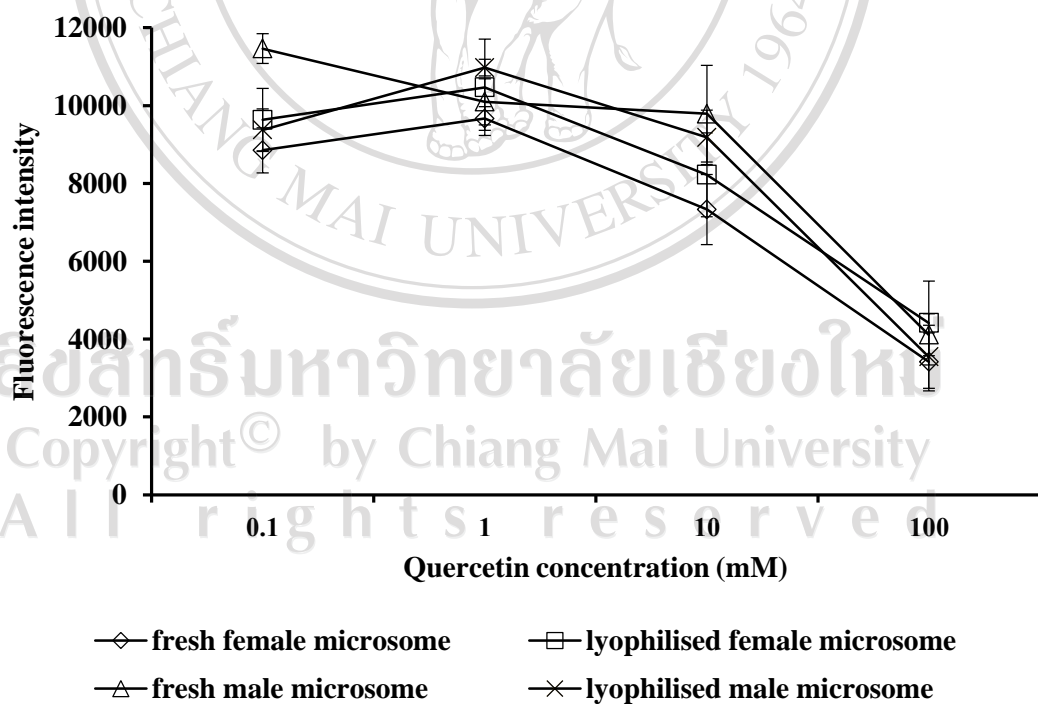


Figure 3.4 The effect of quercetin on fluorescence intensity both in freshly prepared and lyophilized microsome from male and female Nile tilapia.

Similarly to those using in freshly prepared and lyophilized form, it was found that lyophilized female microsome is proper for long term studying by the reason of to ensure that fish has never been masculinized or exposed to masculinizing agent. However, the effect of pH on microsomal enzyme was study. The pH of fish blood is fluctuated due to species variation, environment, electrolytes, temperature, and stress. Therefore, the enzyme activity was examined in different pH (Burton, 1996; Evans, 1998). The results were shown in Figure 3.5.

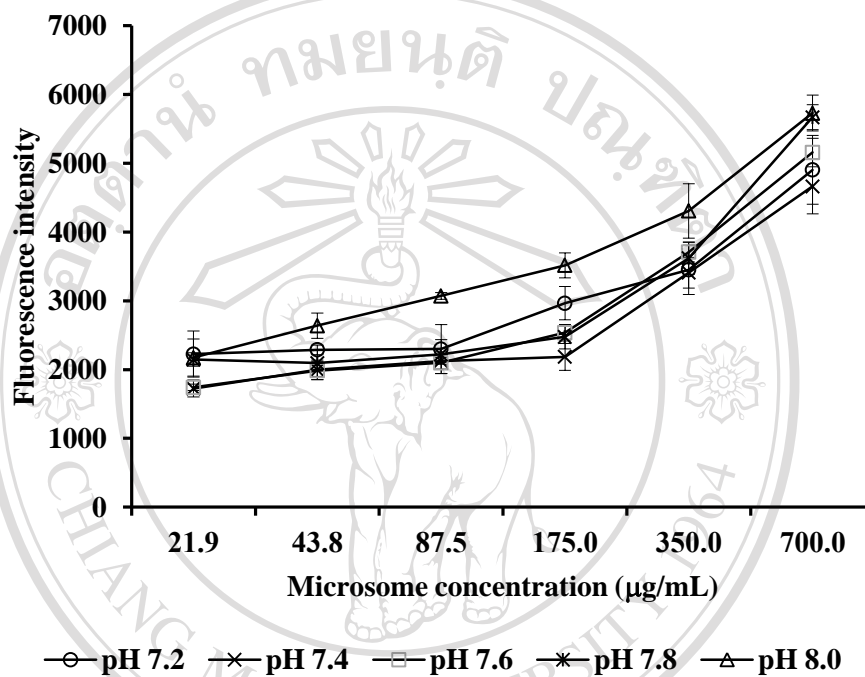


Figure 3.5 The effect of pH on aromatase activity in various concentration of microsome protein

The aromatase activity of the fish microsomes dissolved in a medium pH 7.2-7.8 was significantly lower than that in pH 8.0. It was noted that at microsome concentrations of 21.9-175 µg/mL, the activity of the enzyme was dose independent. The complete dose dependent activity was found only when the enzyme was in pH 8.0. Therefore, the medium pH 8.0 was considered to be the most effective for aromatase activity of Nile tilapia microsomes and this pH was chosen for using in the further study at concentration of 350 µg/mL.

To examined the effected of flavonoids on aromatase inhibitory activity, various flavonoids were applied to this conditions. The results of flavonoids on various concentration were shown in Figure 3.6.

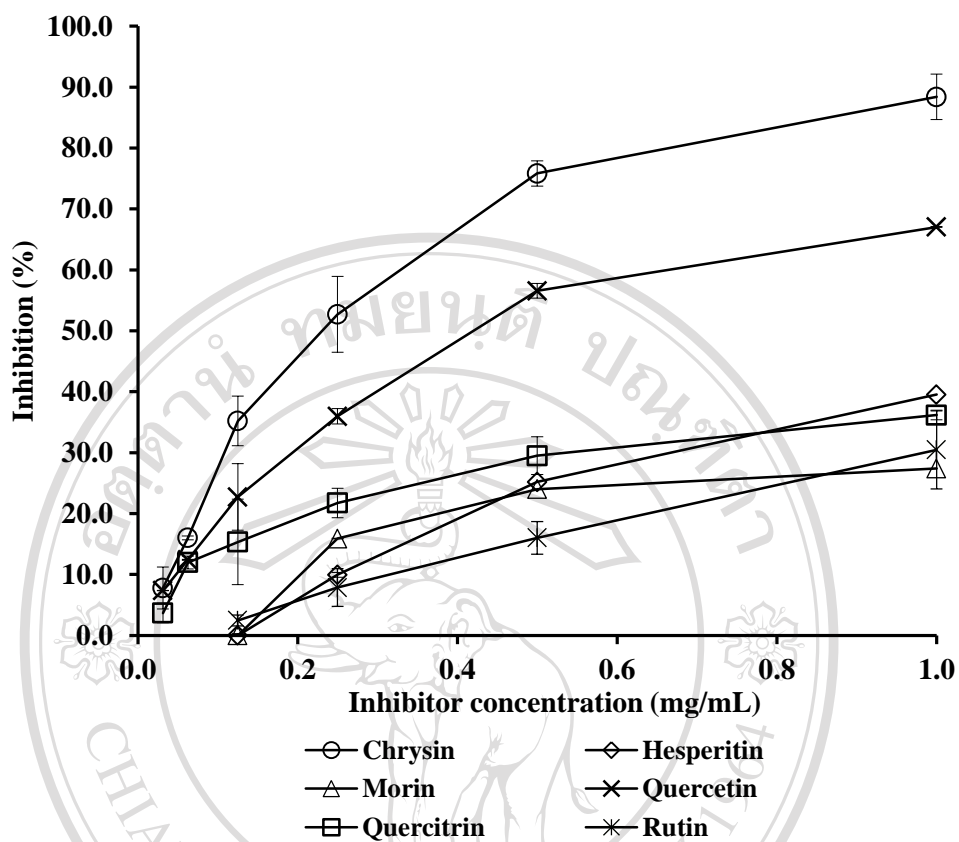


Figure 3.6 The effect of increasing concentrations of hesperidine, morin, quercetin, quercitrin, and rutin on aromatase inhibition

All compounds could inhibit the aromatase activity of Nile tilapia microsomes as a dose dependent activity but in different levels as seen in Figure 3.6. Among them, chrysin showed the highest anti-aromatase activity with the  $IC_{50}$  value of 0.25 mg/mL, approximately 2 times higher than quercetin. The result also indicated the effects of structure activity relationship of the compounds. Substitution of OH group to chrysin, such as in quercetin molecule, caused significant decrease in antiaromatase activity. In addition, consideration between a flavonoid quercetin and its glycoside formed from deoxyrhamnose substitution, quercitrin, resulted that the aglycone quercetin possessed higher activity than its corresponding glycoside, quercitrin. Since the active site of aromatase is highly hydrophobic (Bonfield, 2012), therefore the compounds with alkyl

or higher hydrophobic aromatic groups could have higher affinity to this enzyme leading to a higher efficiently block enzyme activity. Substitution with OH group or sugar moieties into chrysin molecule can decrease its hydrophobicity. Therefore, chrysin with the highest hydrophobicity among the tested compounds showed the highest potency of antiaromatase activity.

The optimal conditions kinetics of enzyme were also examined in female liver microsome. The  $V_{\max}$  and  $K_m$  were also studied and the result was reveal in Figure 3.7.

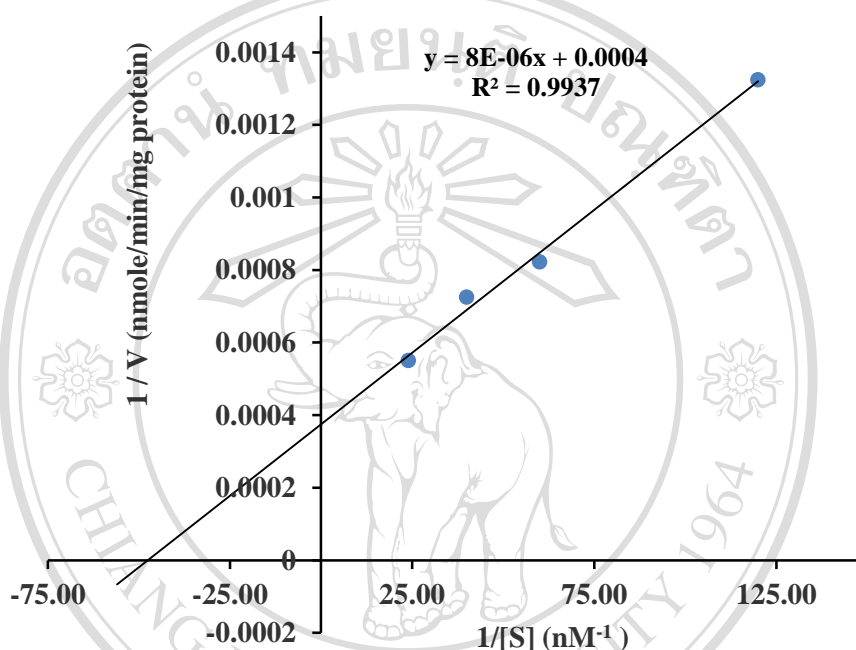


Figure 3.7 Lineweaver-Burk plot for  $K_m$  and  $V_{\max}$  values of the aromatase in the presence of different concentrations of dibenzylfluorescence.

The Lineweaver-Burk plot reveal the straight line that allow  $K_m$  and  $V_{\max}$  as the intercept on the x-axis is equal to  $-1/K_m$  and the intercept on the y-axis is equal to  $1/V_{\max}$ . Determined  $V_{\max}$  and  $K_m$  values of female fish liver aromatase using Lineweaver-Burk graph has calculated  $149.97 \pm 0.05$  nmole/min/mg protein intensity/min/mg protein and  $0.02 \pm 0.01$   $\mu\text{M}$ , respectively. Addition of 2 M NaOH at the end of the reaction resulted in fluorescence intensity increasing 1.2-1.4 fold. It is feasible to detect activity of aromatase without using of 2 M of NaOH. The fluorescence intensity of DBF declined to the steady-state value during 10-minute initial measurement similar to the results of Salminen (2011). The effect of 22 ethanolic

extracts were determined by optimal conditions. There are some different slope value and pattern of inhibitory activity as revealed in Figure 3.8-3.29.

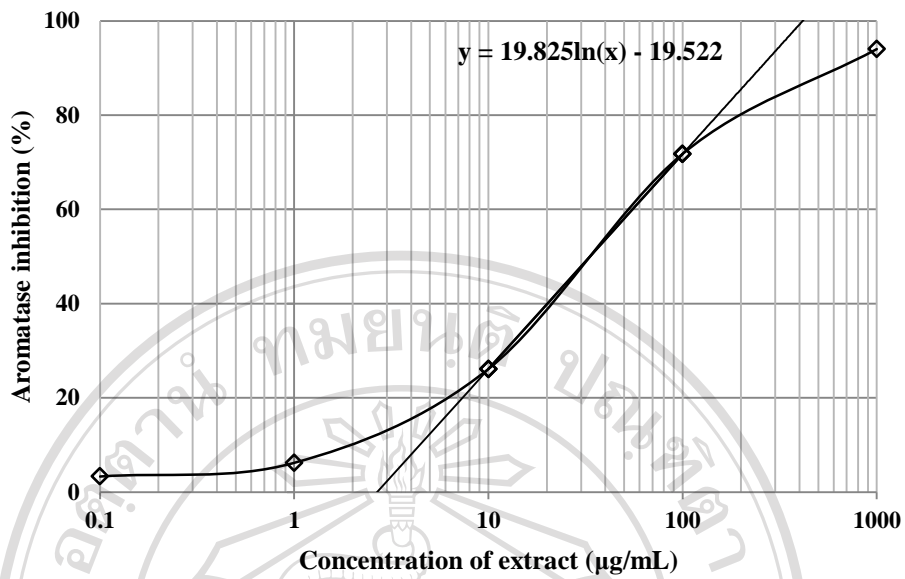


Figure 3.8 The dose-response curve of aromatase inhibition versus concentration of *Ageratum conyzoides*

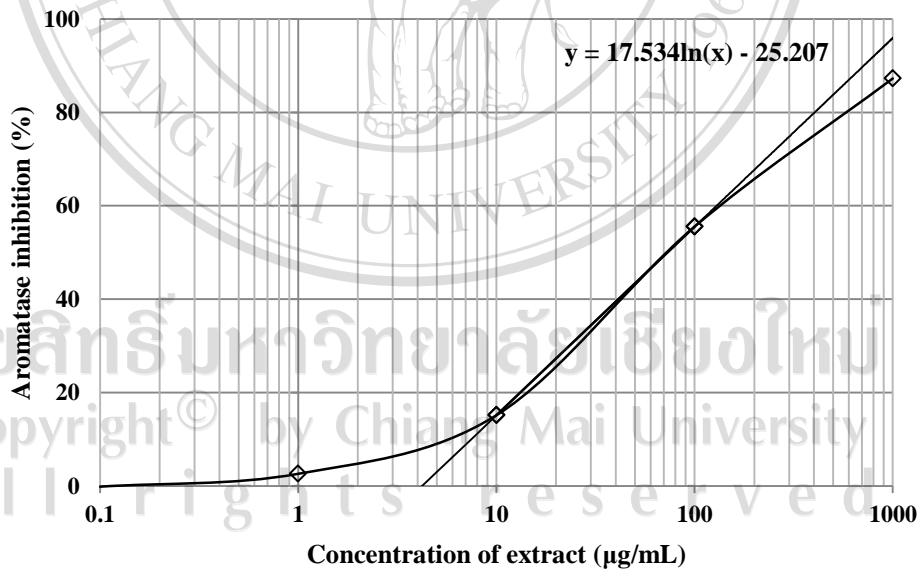


Figure 3.9 The dose-response curve of aromatase inhibition versus concentration of *Allium cepa* var. *aggregatum*

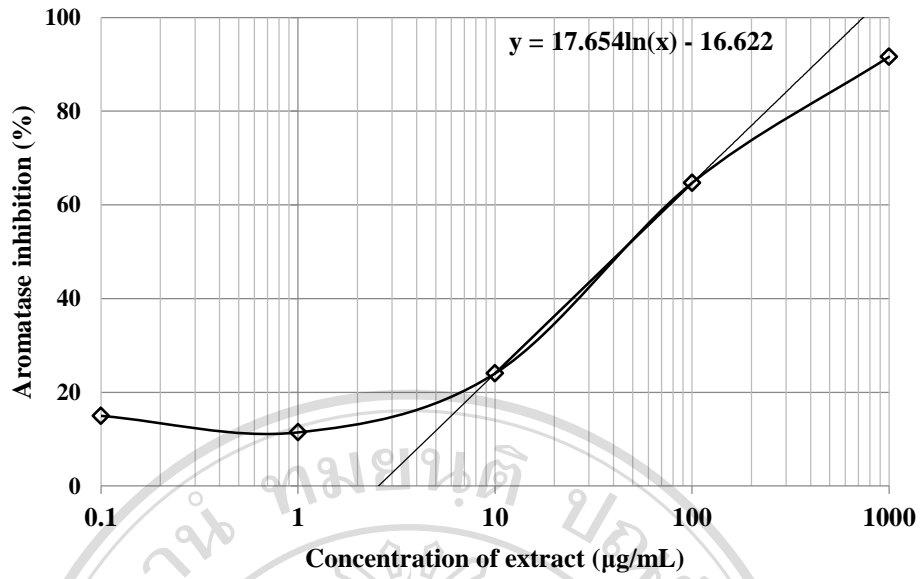


Figure 3.10 The dose-response curve of aromatase inhibition versus concentration of *Artabotrys siamensis*

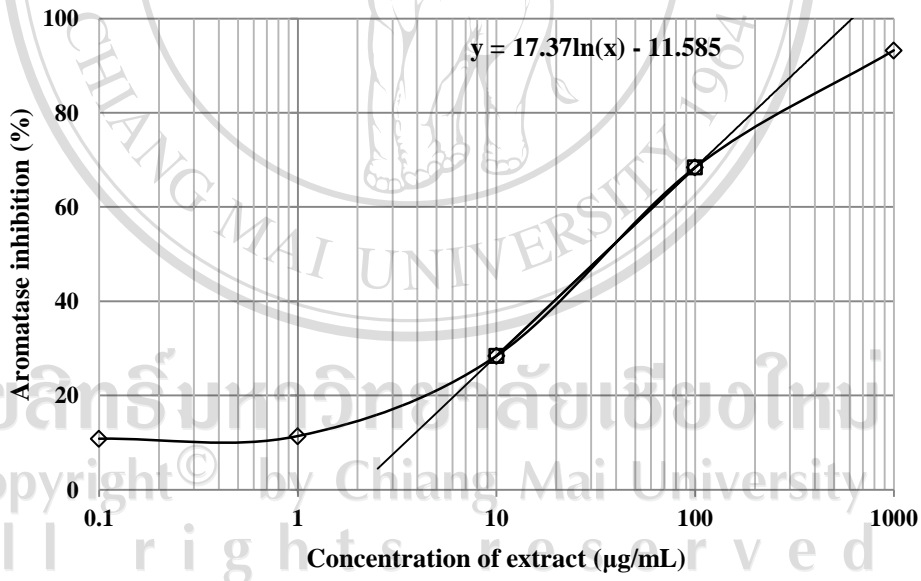


Figure 3.11 The dose-response curve of aromatase inhibition versus concentration of *Cananga odorata*

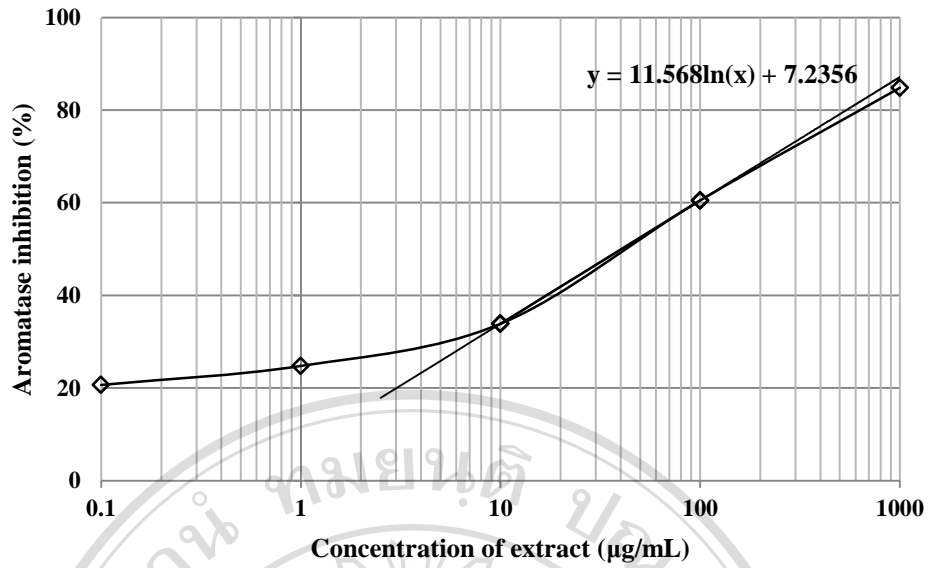


Figure 3.12 The dose-response curve of aromatase inhibition versus concentration of *Catharanthus roseus*

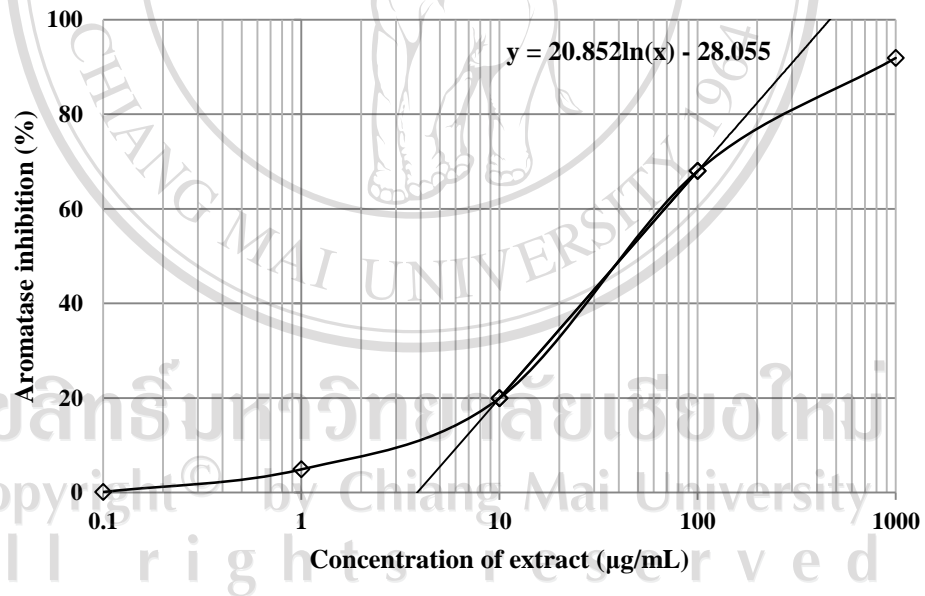


Figure 3.13 The dose-response curve of aromatase inhibition versus concentration of *Cleistocalyx nervosum* var. *paniala*

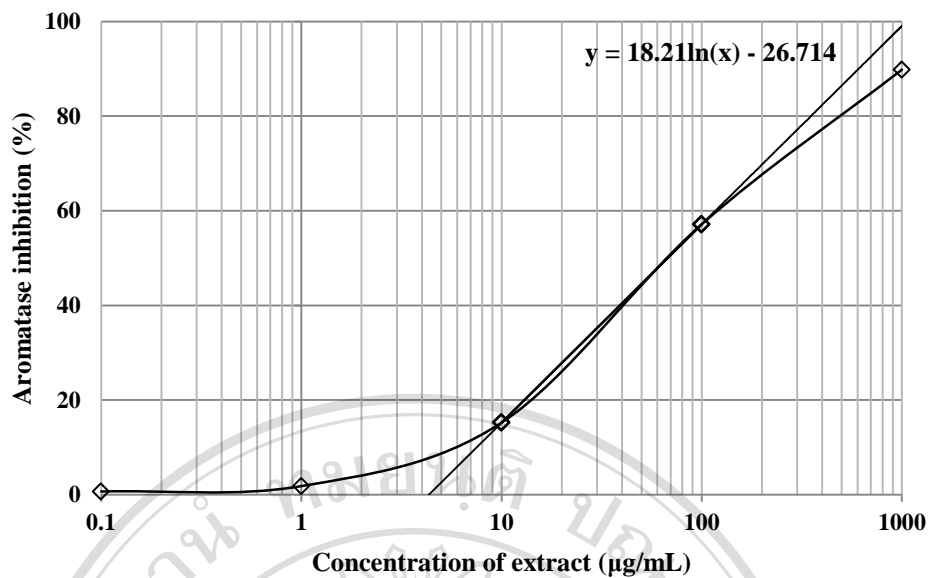


Figure 3.14 The dose-response curve of aromatase inhibition versus concentration of *Coriandrum sativum*

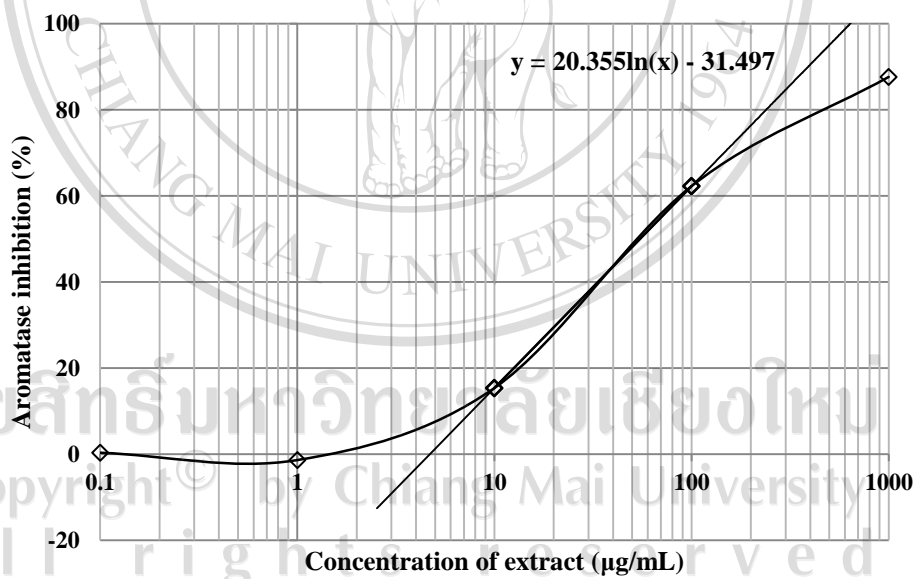


Figure 3.15 The dose-response curve of aromatase inhibition versus concentration of *Cycas revolute*

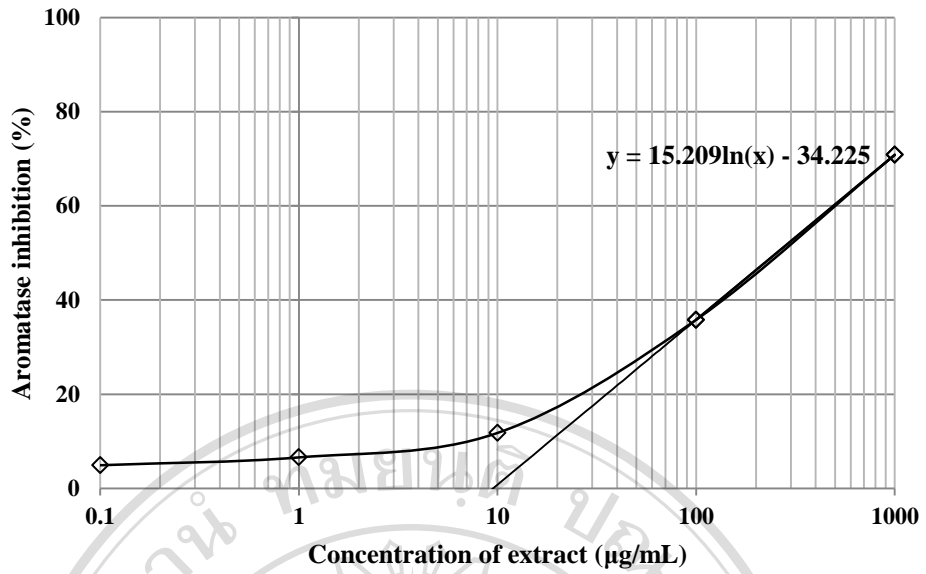


Figure 3.16 The dose-response curve of aromatase inhibition versus concentration of *Dolichos Lablab*

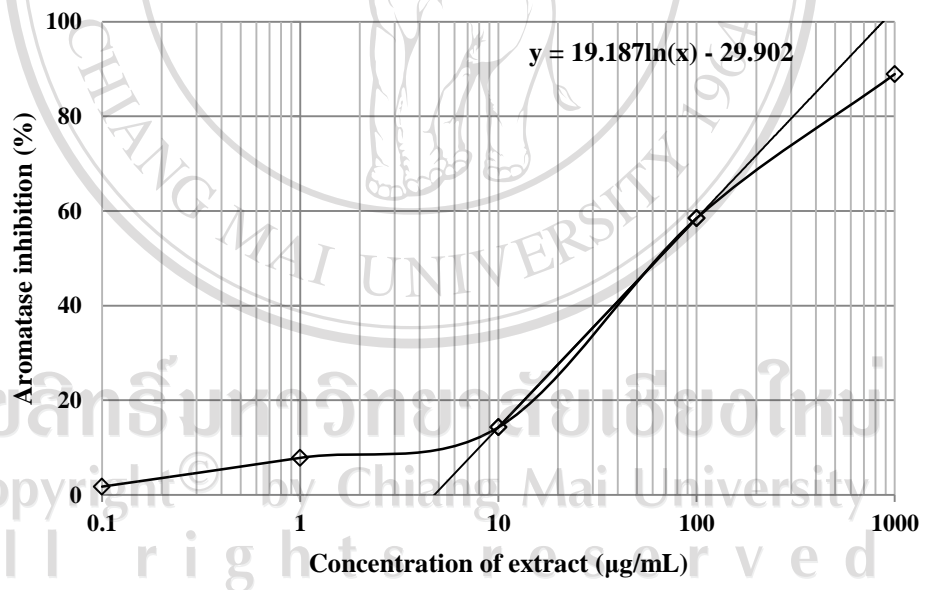


Figure 3.17 The dose-response curve of aromatase inhibition versus concentration of *Millingtonia hortensis*

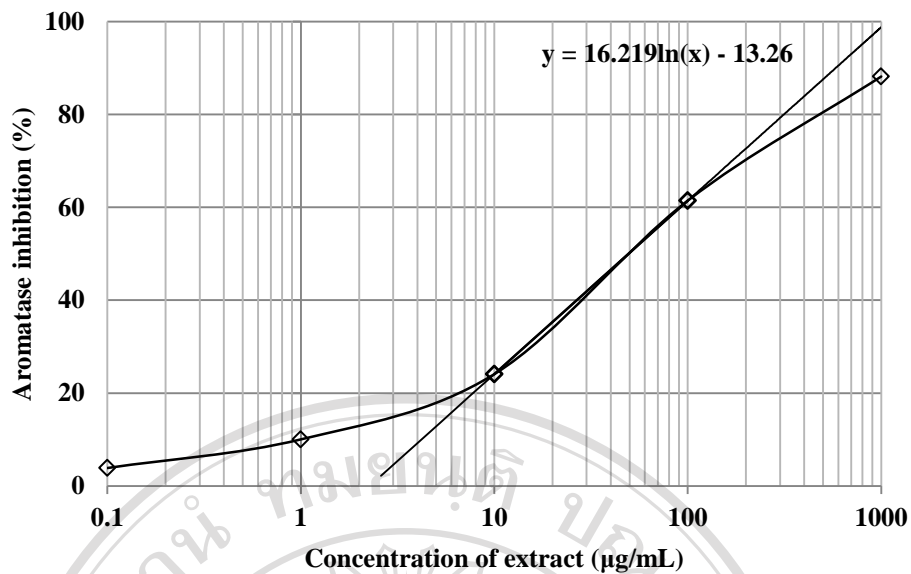


Figure 3.18 The dose-response curve of aromatase inhibition versus concentration of *Mimusops elengi*

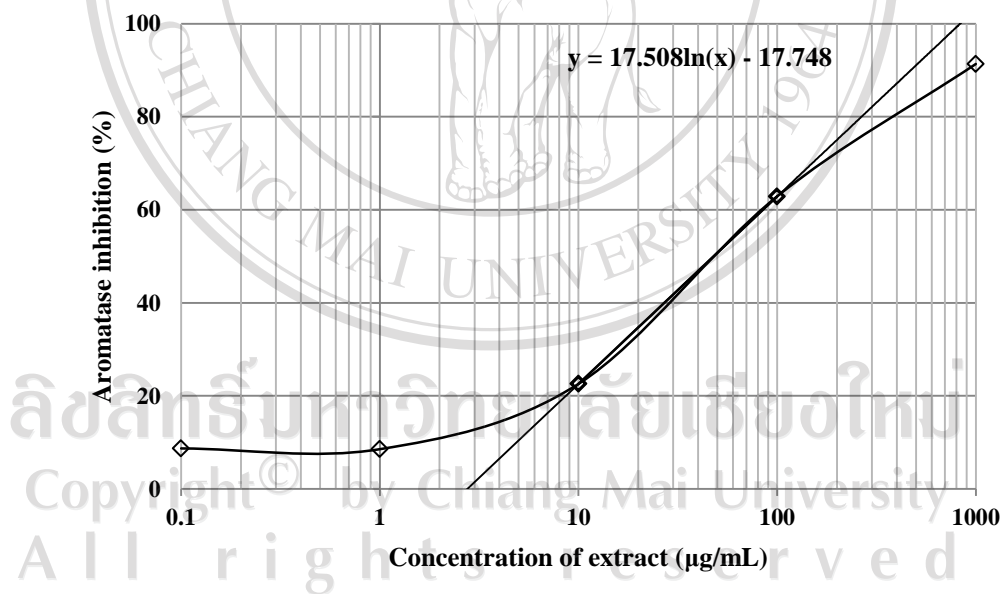


Figure 3.19 The dose-response curve of aromatase inhibition versus concentration of *Momordica charantia*

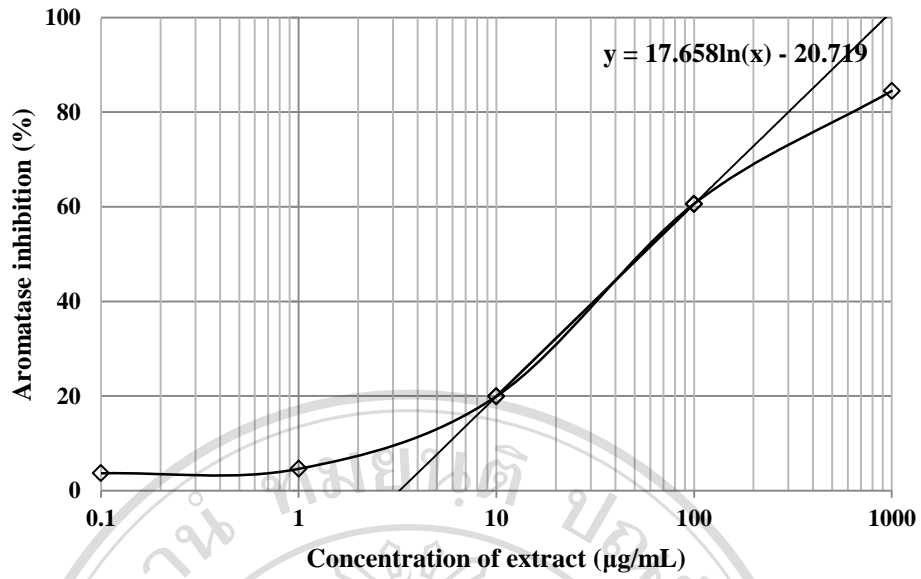


Figure 3.20 The dose-response curve of aromatase inhibition versus concentration of *Moringa oleifera*

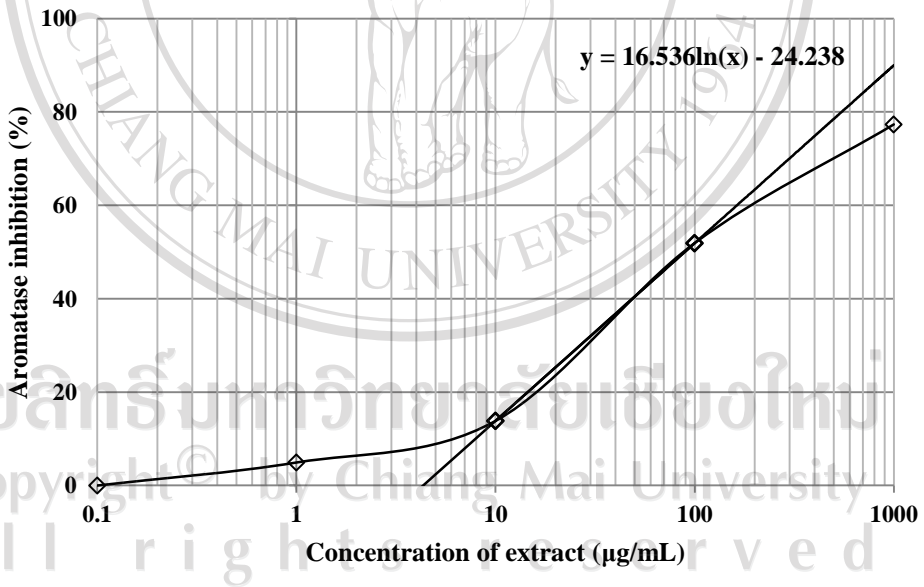


Figure 3.21 The dose-response curve of aromatase inhibition versus concentration of *Nymphaea nouchali*

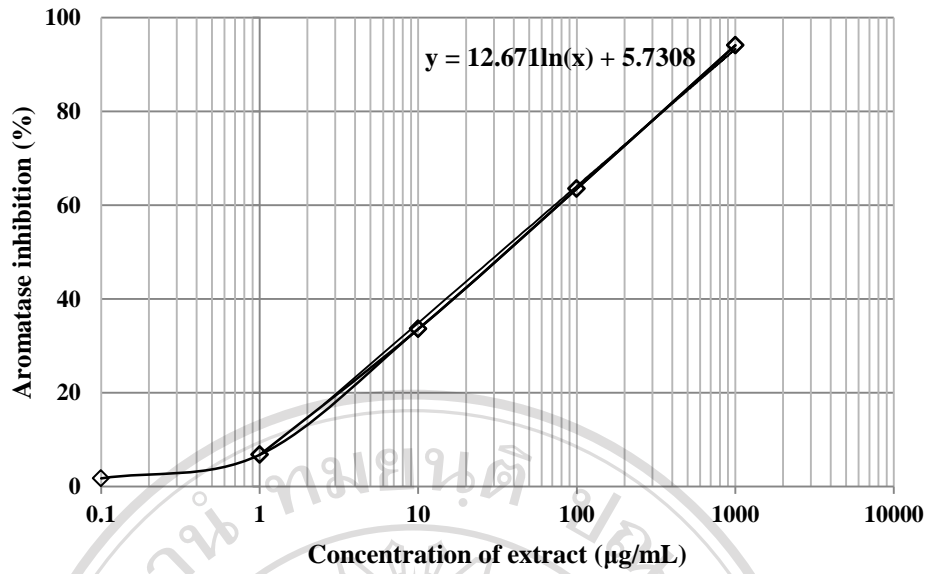


Figure 3.22 The dose-response curve of aromatase inhibition versus concentration of *Oroxyllum indicum*

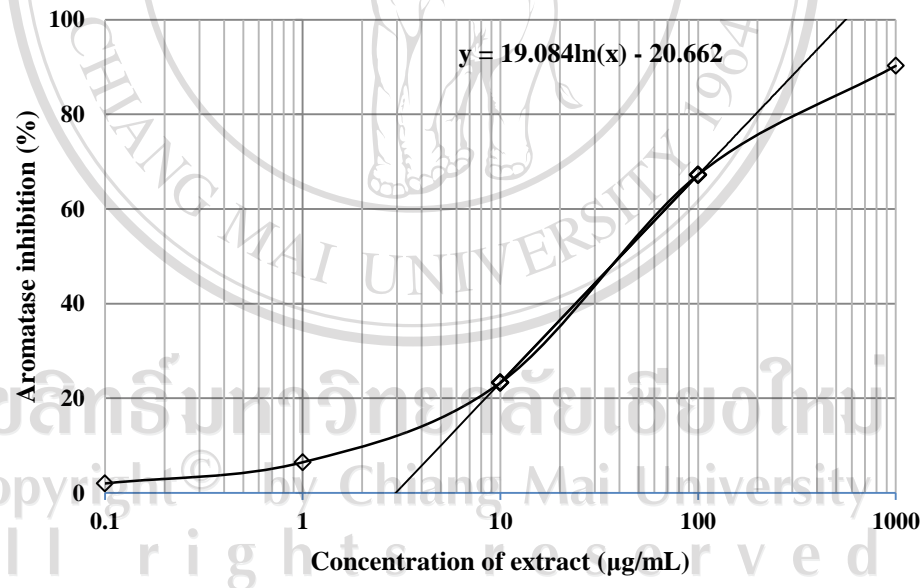


Figure 3.23 The dose-response curve of aromatase inhibition versus concentration of *Passiflora edulis*

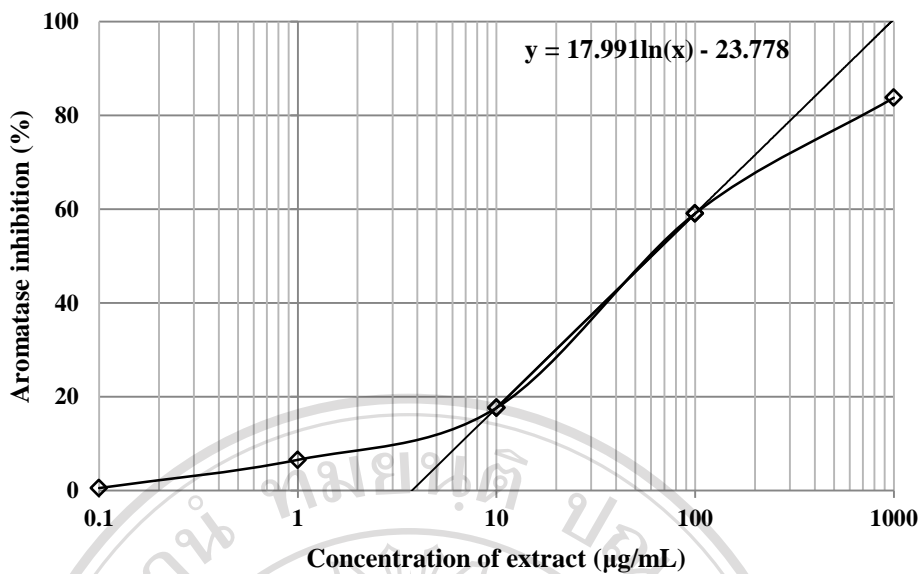


Figure 3.24 The dose-response curve of aromatase inhibition versus concentration of *Passiflora foetida*

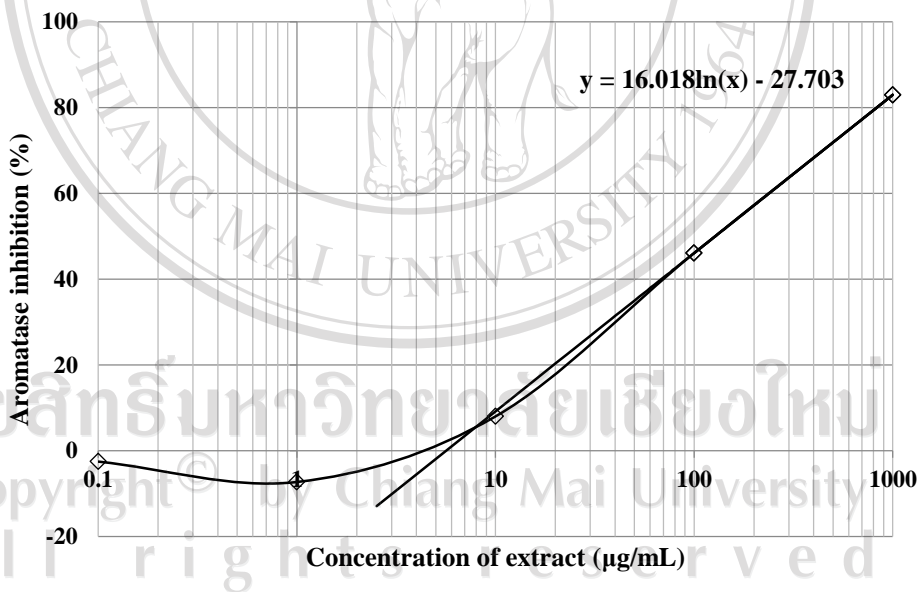


Figure 3.25 The dose-response curve of aromatase inhibition versus concentration of *Plantago major*

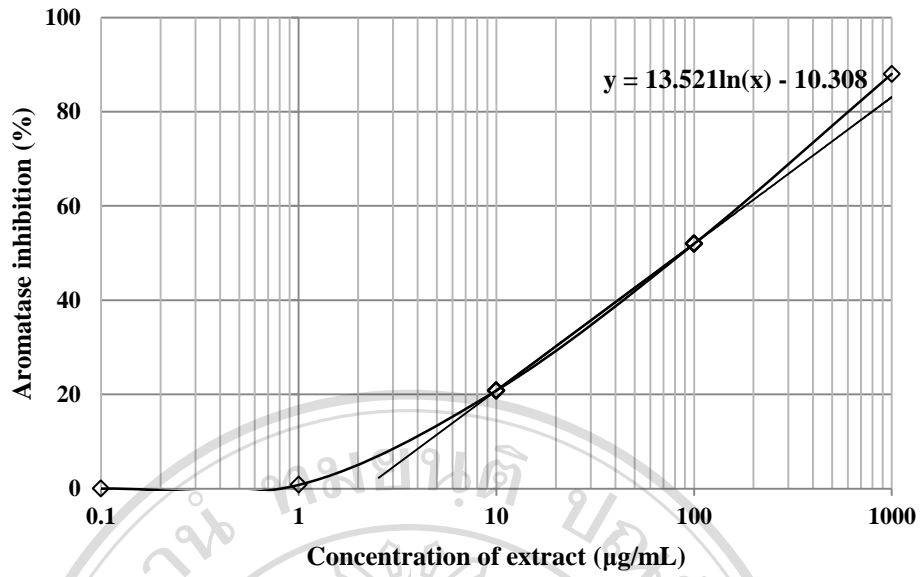


Figure 3.26 The dose-response curve of aromatase inhibition versus concentration of *Punica granatum*

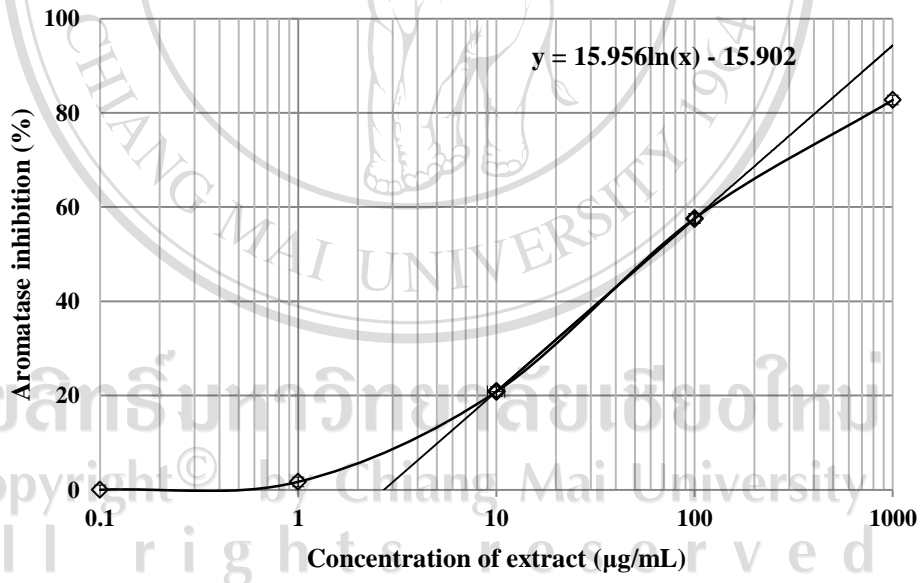


Figure 3.27 The dose-response curve of aromatase inhibition versus concentration of *Spondias pinnata*

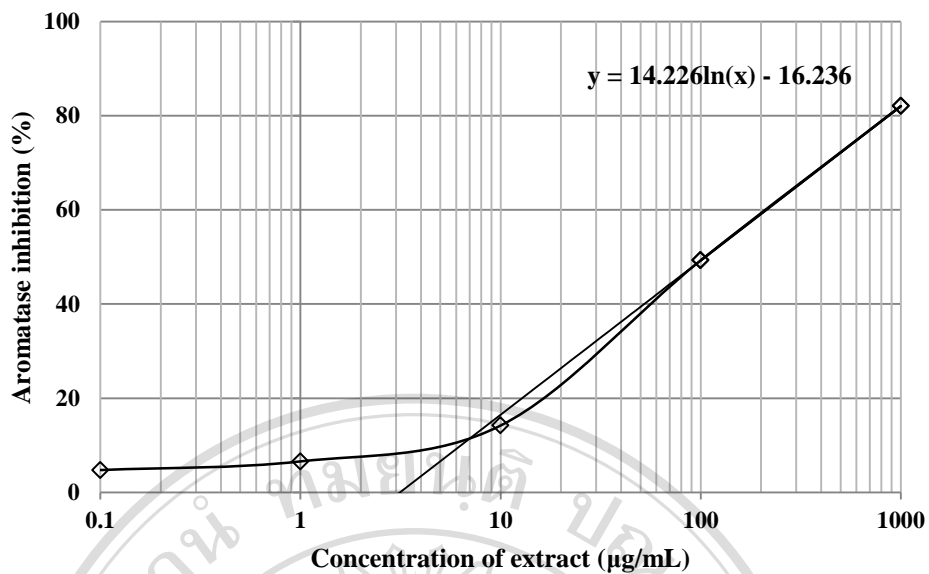


Figure 3.28 The dose-response curve of aromatase inhibition versus concentration of *Terminalia catappa*

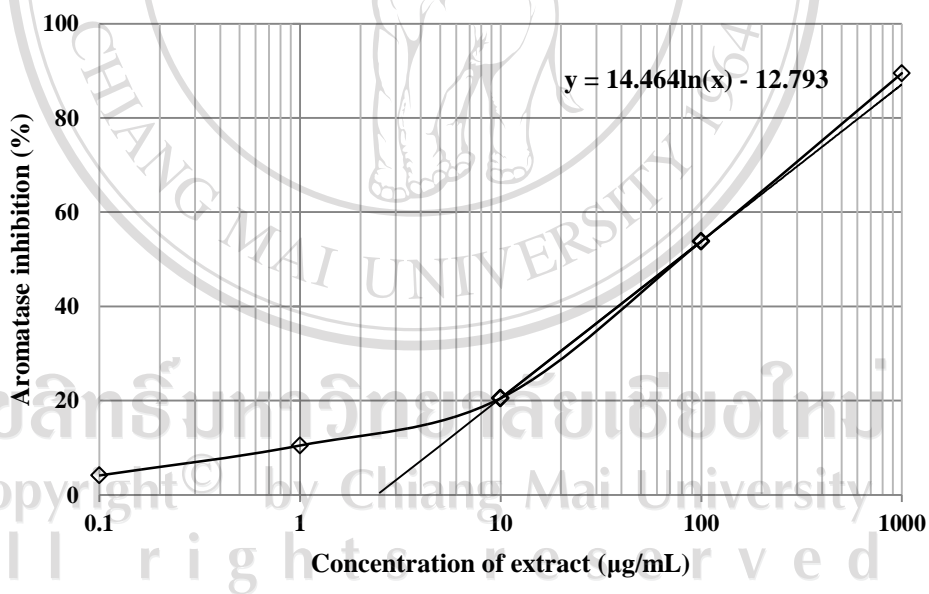


Figure 3.29 The dose-response curve of aromatase inhibition versus concentration of *Wrightia religiosa*

The finding in this study is *O. indicum* revealed the dose-response inhibition curve at the lowest concentration, 10 µg/mL of *O. indicum* extract versus aromatase inhibition. It revealed highest potent compared to the others extracts at the same concentration. Thus, the IC<sub>50</sub> value of each sample was calculated by the linear curve equation. The IC<sub>50</sub> of DBF metabolism by plant extracts were showed in Figure 3.30.

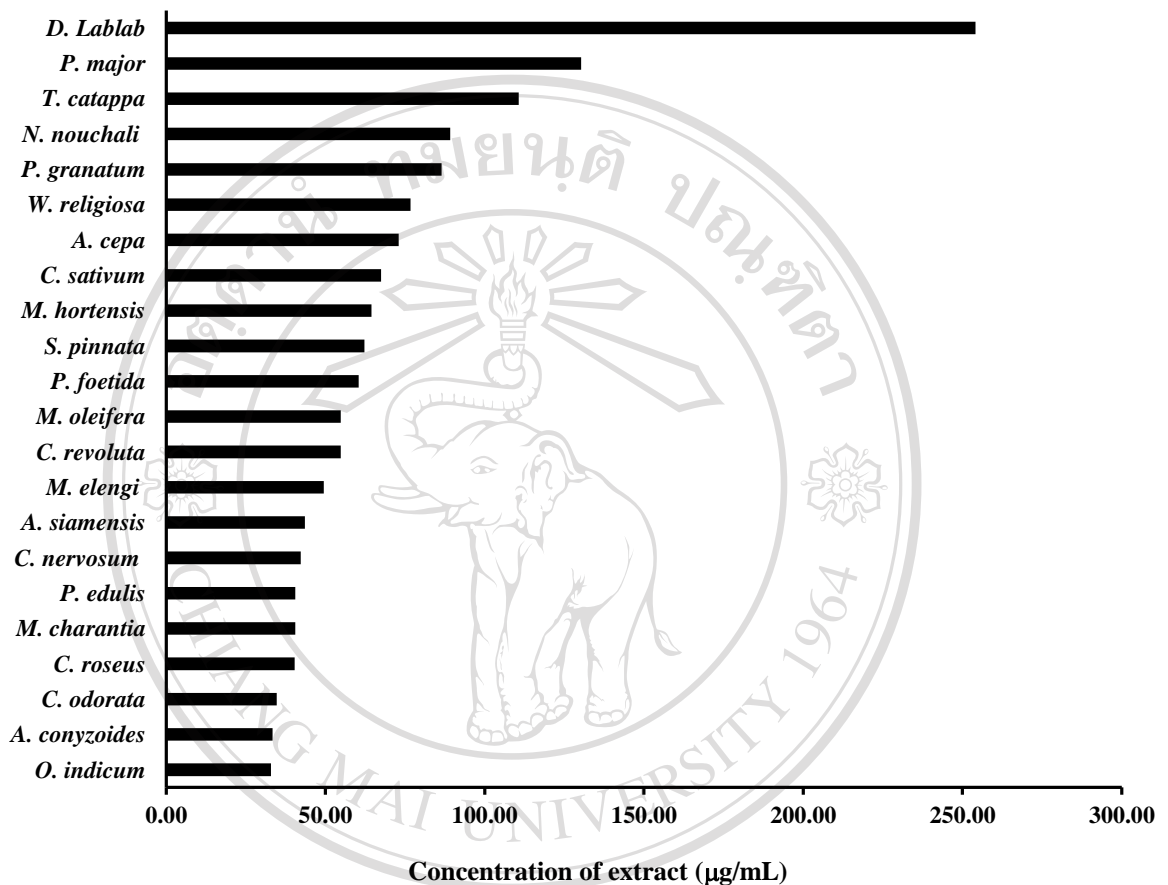


Figure 3.30 The IC<sub>50</sub> of ethanolic plant extracts

The finding indicated that *O. indicum*, *A. conyzoides* and *C. odorata* had the highest potent in inhabiting aromatase activities. The best plant extract was selected based-on the smallest amount of flavonoid composition used to reach the same IC<sub>50</sub> value. The flavonoid content assay was performed and shown in the Figure 3.31.

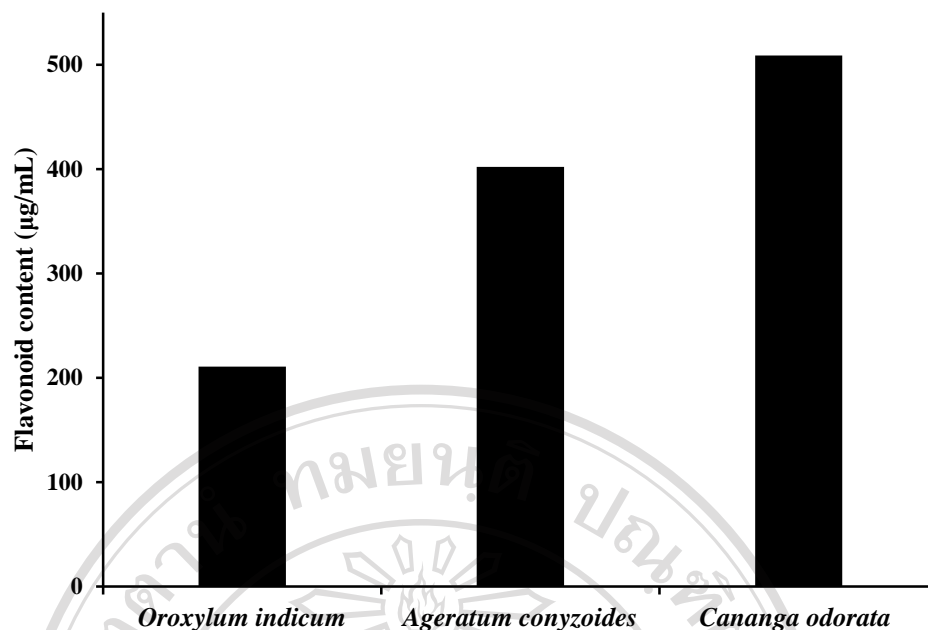


Figure 3.31 The flavonoid content of *O. indicum*, *A. conyzoides* and *C. odorata*

It can be concluded that the small amount of flavonoid content in *O. indicum* extract possess the most potent to inhibit aromatase activity at the same  $IC_{50}$  value. Moreover, some researcher found that coumarin in *A. conyzoides* is moderately toxic to the liver and kidneys can metabolize form of coumarin is hepatotoxic in rats, unstable compound that on further differential metabolism may cause liver cancer and lung tumors in animals (Vassallo, 2004; Born, 2003) whereas *C. odorata* was also never been proven for oral route administration.

For those reason, *O. indicum* was fractionated by using hexane, ethyl acetate and ethanol, respectively. All fractions were tested for cytotoxicity in sex hormone sensitive cell lines, HepG2 and MCF-7. The results were shown in Figure 3.32.

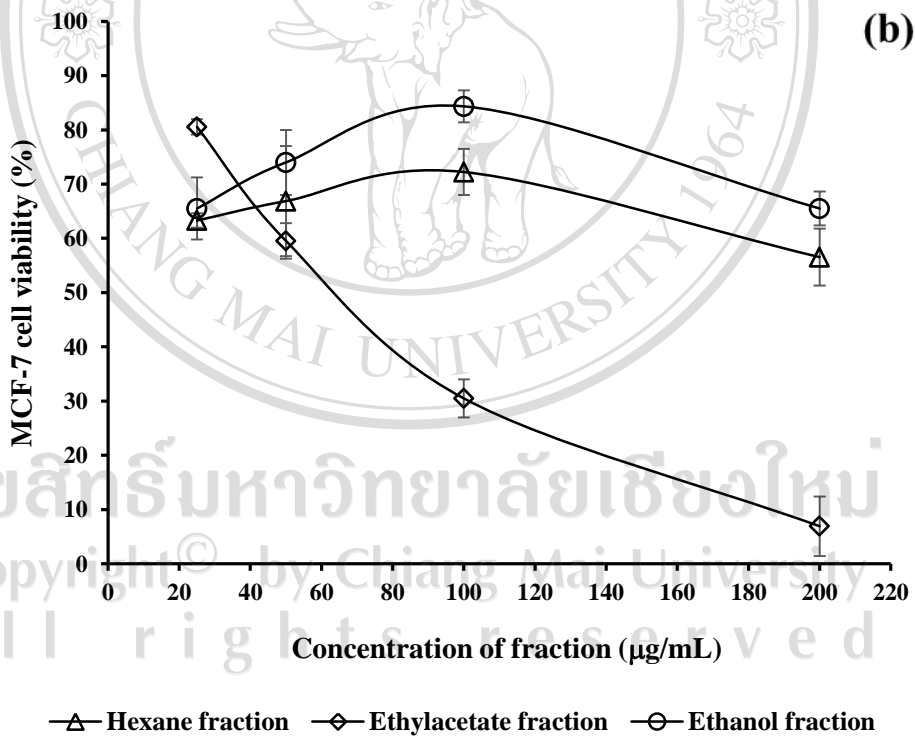
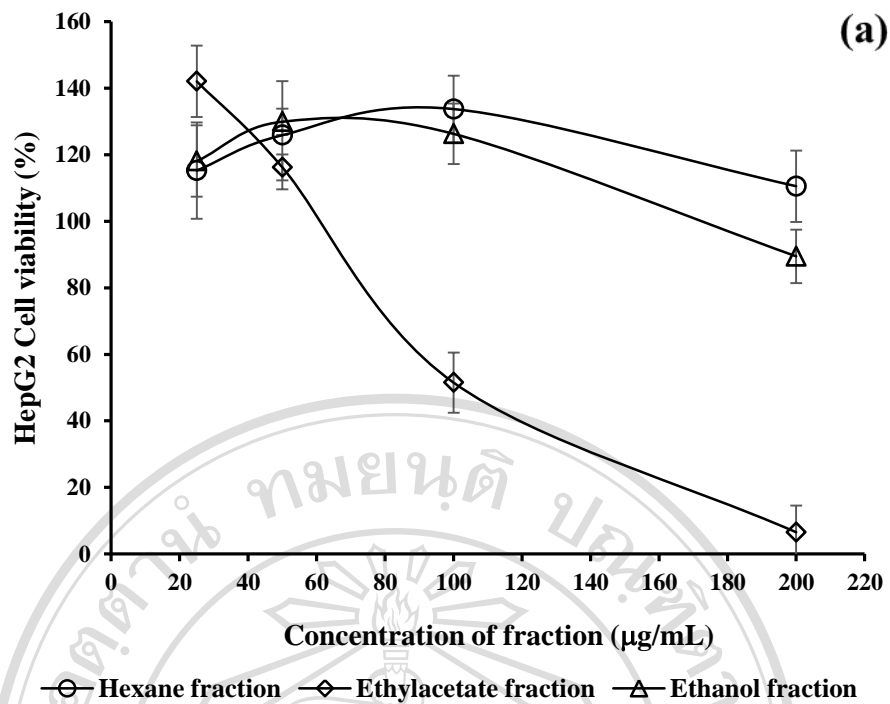


Figure 3.32 The cytotoxicity of fractionate of *O. indicum* against HepG2 (a) and MCF-7 (b)

It was found that ethyl acetate fraction of *O. indicum* possess highest cytotoxicity against both HepG2 and MCF-7 cell lines. Thus, to examine the active compound, The 1 mg/mL of each fraction was identified by using HPLC. The result of chromatogram was revealed in Figure 3.33.

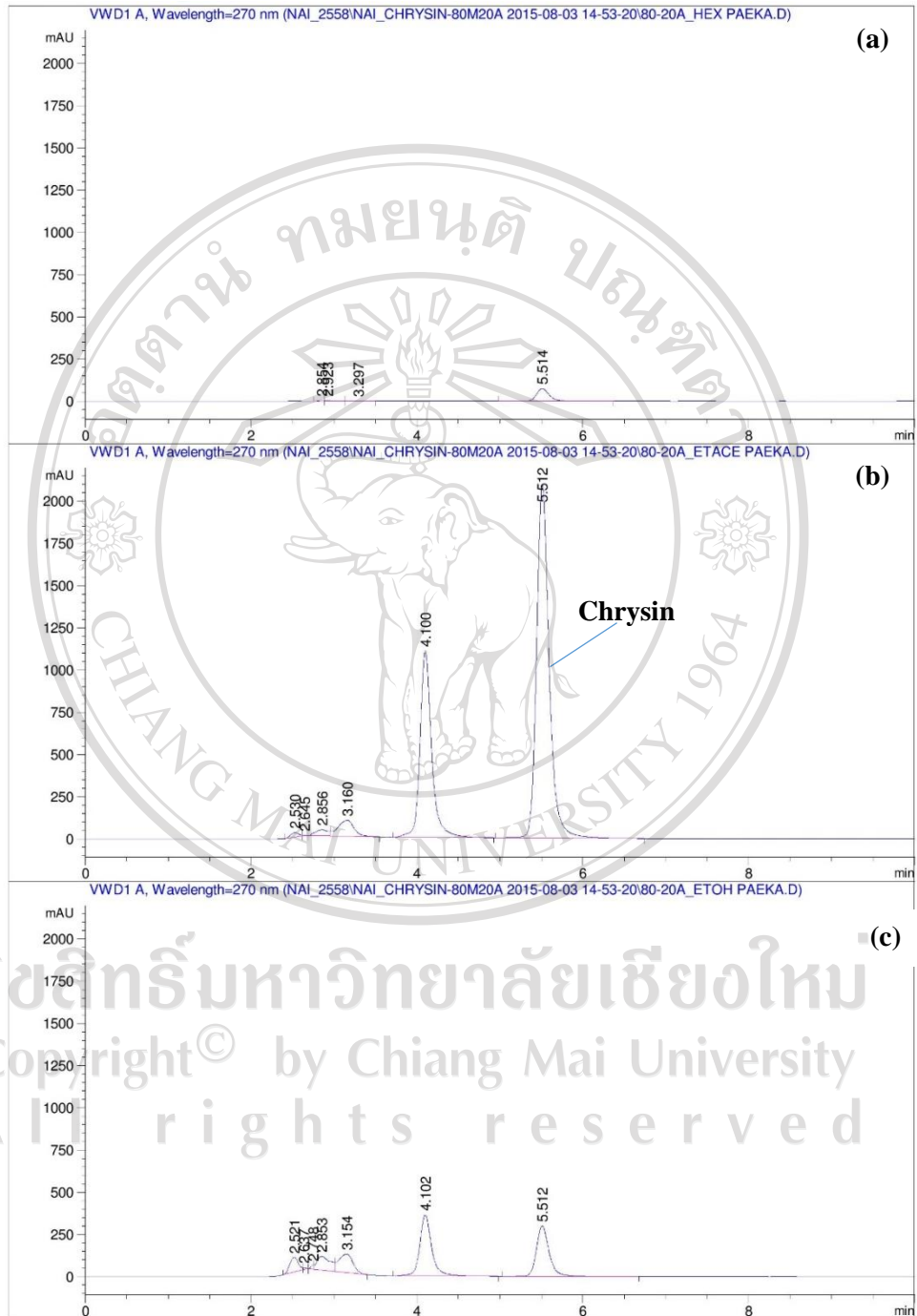


Figure 3.33 The chromatogram of hexane (a), and ethyl acetate (b), and ethanol (c) fractions

The HPLC profile of EtOAc fraction under UV 270 nm was recorded. The fraction revealed major peaks with retention time (RT) values of 5.5 minute for 10  $\mu$ L application volume. The isocratic solvent, methanol:deionized water (80:20), was used as mobile phase in C-18 column. The chromatogram revealed that chrysin was the major compound in the fraction compared to chrysin standard as indicated in appendix C.

From all results, It can be concluded that chrysin in *O.indicum* has the higher potent of aromatase inhibition activity than the other extracts on microsome system. The  $IC_{50}$  of chrysin, ethyl acetate fraction and crude extract of *O.indicum* were compared in Figure 3.34.

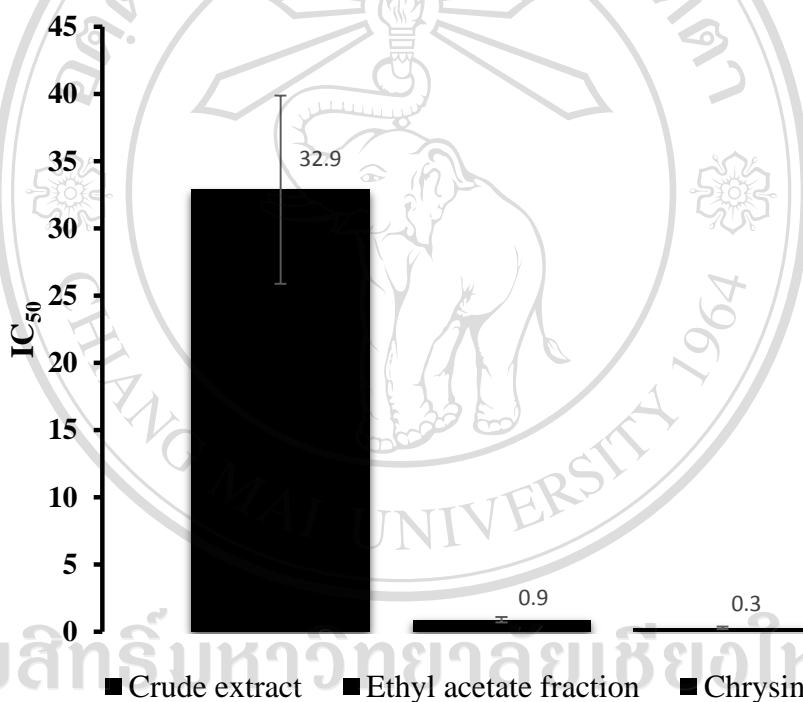


Figure 3.34 The comparison of  $IC_{50}$  of 1 mg/mL of the crude extract, ethyl acetate fraction, and chrysin.

The purified compound, chrysin, showed the highest inhibitory effect on fish aromatase microsome system compared to crude extract and ethyl acetate fraction about 109.7-fold and 3-fold, respectively. Unfortunately, chrysin is insoluble compound.

Thus, to increase the solubility, chrysin was entrapped by various polymer and surfactant for drug delivery into fish target cells.



ลิขสิทธิ์มหาวิทยาลัยเชียงใหม่  
Copyright© by Chiang Mai University  
All rights reserved

## Part III Development of nanochrysin entrapment

### 1. HP $\beta$ CD entrapment

It was found that, after re-suspending the nanoparticle with deionized water, nanoparticles as chrysin loaded HP $\beta$ CD were obtained from the formulation which adding 200-300  $\mu$ L of tween 20 and tween 80. The unimodal histogram were shown in the Figure 3.35 and the zeta potential peaks were shown in Figure 3.36.

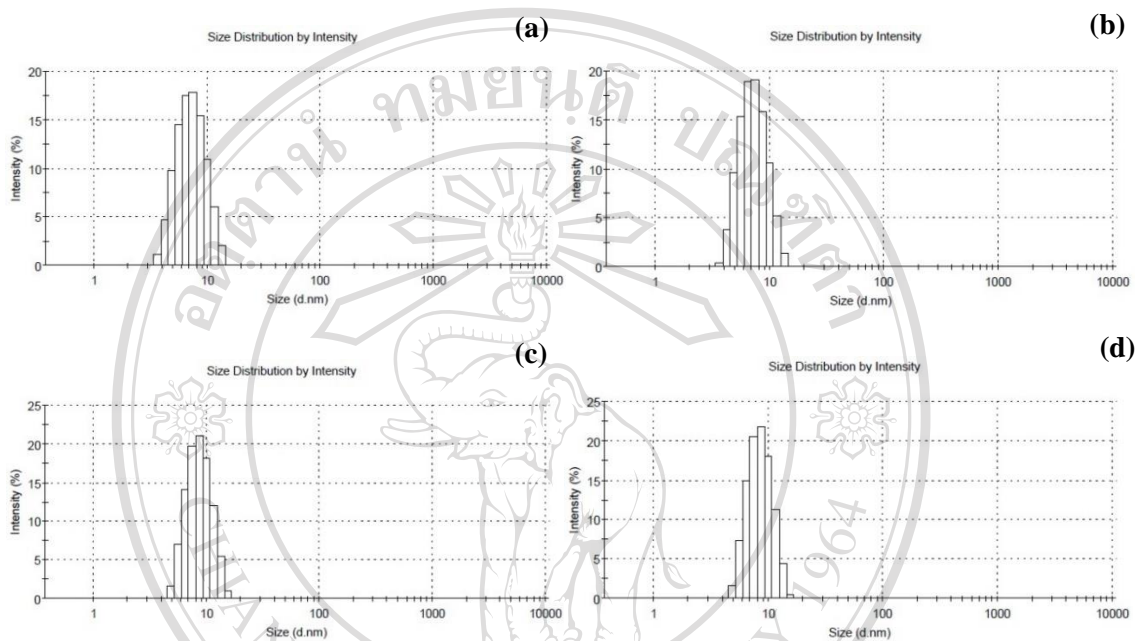


Figure 3.35 The histogram of chrysin loaded HP $\beta$ CD made from Chrysin :HP $\beta$ CD : Tween 20 in ratio (a) 1:1:200 (mole:mole: $\mu$ L) (b) 1:1:300 (mole:mole: $\mu$ L) and Chrysin:HP $\beta$ CD:Tween 80 in ratio (c) 1:1:200 (mole:mole: $\mu$ L) (d) 1:1:300 (mole:mole: $\mu$ L)

Chrysin was entrapped by HP $\beta$ CD with stoichiometry 1:1. The interaction between the complex occurred by the A-ring of the chrysin interacted into hydrophobic side of HP $\beta$ CD (Chakraborty, 2010). The nanosize of the chrysin loaded HP $\beta$ CD coated by Tween 20 was smaller than coated by Tween 80 but not significantly. However, the PDI indicated that the chrysin loaded HP $\beta$ CD coated by Tween 80 is narrower than coated by Tween 20.

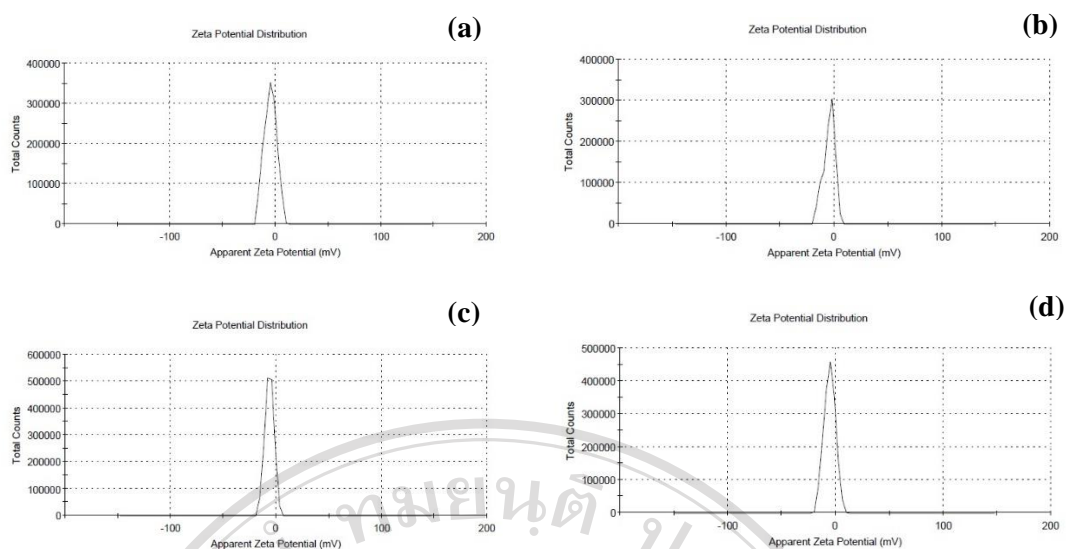


Figure 3.36 The zeta potentials of chrysin loaded HP $\beta$ CD made from Chrysin :HP $\beta$ CD : Tween 20 in ratio (a) 1:1:200 (mole:mole: $\mu$ L) (b) 1:1:300 (mole:mole: $\mu$ L) and Chrysin :HP $\beta$ CD : Tween 80 in ratio (c) 1:1:200 (mole:mole: $\mu$ L) (d) 1:1:300 (mole:mole: $\mu$ L)

The zeta potentials of all formulations were nearly zero mV due to the effect of non-ionic surfactant on surface charge of particles. However, the particles were in formed in gel- type resulted no precipitation occurred in the solution. The summarization of each formulation was revealed in Table 3.3.

Table 3.3 The characteristics of chrysin loaded nanoparticles obtained from the use of HP $\beta$ CD as oligomer and tween 20, tween 80 as surfactants

Surfactants (per 1 mg of chrysin)	Volume ( $\mu$ L)	size (nm)	PDI	Intensity (%)	% EE
Tween 20	100	ND	ND	ND	ND
	200	$7.452 \pm 2.209$	$0.060 \pm 0.01$	100	100
	300	$7.399 \pm 2.049$	$0.051 \pm 0.01$	100	100
Tween 80	100	ND	ND	ND	ND
	200	$8.684 \pm 2.243$	$0.039 \pm 0.01$	100	100
	300	$8.684 \pm 2.116$	$0.040 \pm 0.01$	100	100

ND = not detectable.

The results indicated that chrysin loaded HP $\beta$ CD were obtained by using HP $\beta$ CD in cooperated with tween 20 or tween 80 (at concentration of at least 200  $\mu$ L/mg chrysin). The increasing of surfactant had no effect on particle size. The narrow PDI with high intensity were obtained from all conditions. The percentage of entrapment efficiency was also performed by indirect method. It was found that chrysin was entrapped absolutely in nanoparticle size range. However, in cooperated from the chrysin:HP $\beta$ CD:tween 80 in ratio (c) 1:1:200 (mole:mole: $\mu$ L) was chosen due to the function of tween 80 on transporting nanoparticle across blood brain barrier (Sun, 2004). The releasing of chrysin in 10 mM HEPES buffer were done in pH 7.0, 7.6, 7.8 and 8.0. The profiles of releasing were revealed in Figure 3.37.

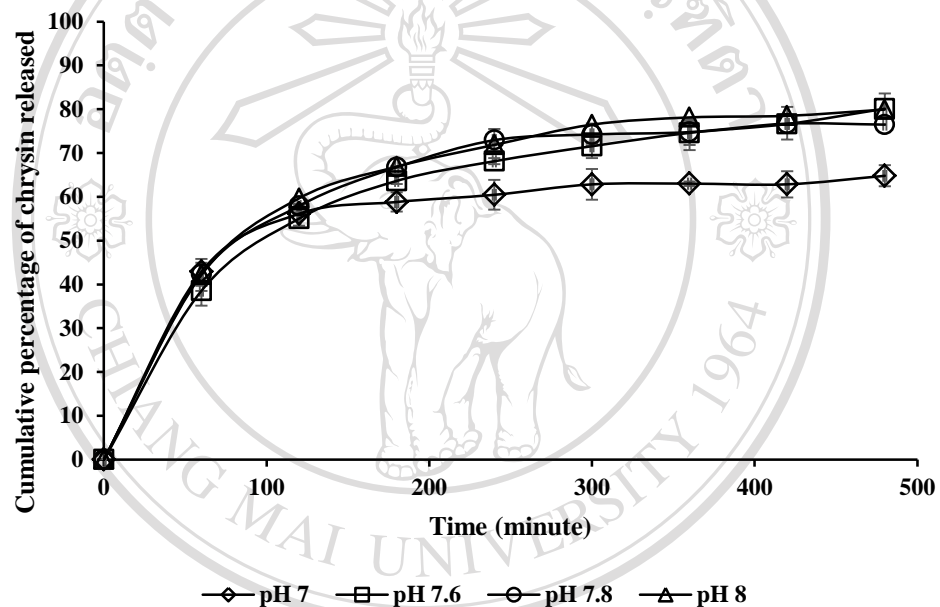


Figure 3.37 The effect of pH on chrysin release behavior from chrysin loaded nanoparticles in 10 mM HEPES buffer.

Figure 3.37 showed *in vitro* chrysin release profiles from nanoparticles prepared by polymeric micelles technology. The percentage of chrysin in 10 mM HEPES buffer, pH 7.0 was reached 60% at 2 hours and the cumulative release had no more increasing within 8 hours. The other conditions of releasing were also done at the same conditions but in different pH. It was also found that pH 7.6, 7.8 and 8.0 revealed the same

behavior of releasing. The percentage of chrysin from polymeric micelles in the same buffer was closely 70% at 3 hours and prolong releasing at the same rate at least 8 hours. It was obvious that chrysin was released from polymeric micelles into water slower than releasing in fish blood circulation.

It is important to know the safe dose or the maximum concentration of chrysin loaded HP $\beta$ CD before approach to the masculinization process. The zebrafish embryo was used as a model for testing toxicity of the developed chrysin loaded HP $\beta$ CD as procedure of Braunbeck (2006). The toxicity results, as the percentage of mortality, of zebrafish embryo was demonstrated in Figure 3.38.

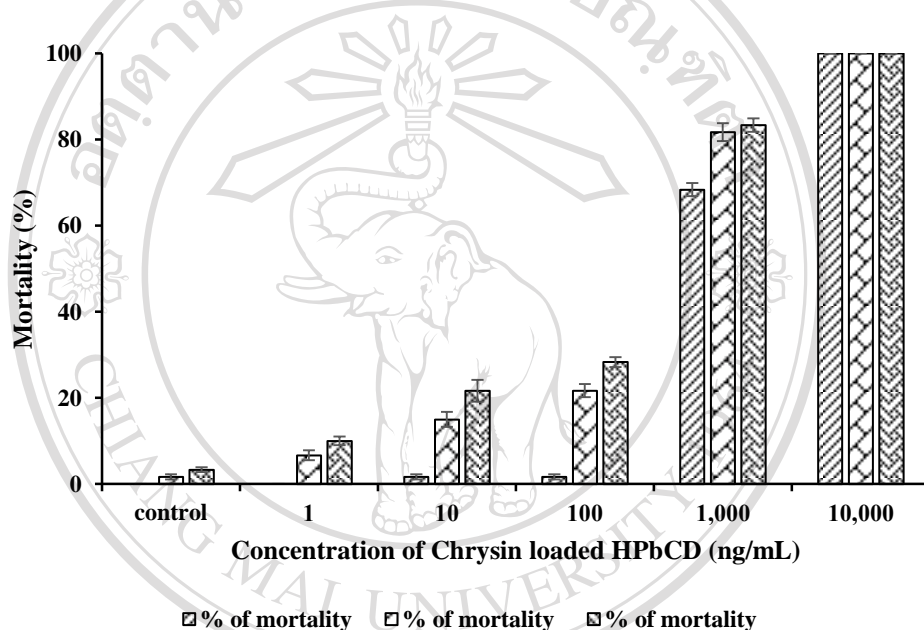


Figure 3.38 The mortality of zebrafish eggs at 24 h, 48 h, and 72 h exposure to chrysin loaded HP $\beta$ CD.

From Figures 3.38, the effect of chrysin loaded HP $\beta$ CD was obviously seen particularly at the low dose range of 1-100 ng/mL, but not significantly different at concentration of 1,000 ng/mL or more. It was found that the toxicity of all samples was seen in a dose dependent manner. The results also showed that the toxic effect of micelles was not time dependent. After incubating zebrafish eggs in the fixed dose

conditions but at different incubation times of 24, 48, and 72 hours, the fish mortality was not significantly different at each dose. The results revealed that zebrafish embryos were died after 24 hours exposure to 10,000 ng/mL whereas more than 70% of the embryos developed normally (without abnormality) after exposure to 1-100 ng/mL. Therefore, the dose range of 10 to 100 ng/mL were selected for further study for zebrafish masculinization.



ลิขสิทธิ์มหาวิทยาลัยเชียงใหม่  
Copyright© by Chiang Mai University  
All rights reserved

## 2. Poloxamer entrapment

In the process of chrysin loaded micelles, Tween 80 has been added for incorporation into the micelles. Tween 80 is a hydrophilic non-ionic surfactant widely used in emulsification and solubilizing of substances in medicinal, pharmaceutical, and food products. Moreover, it is used in conjunction with nanoparticles to improve specific delivery (Sun, 2004). Tween 80 is reported to be adsorbed on the surface by interacting with specific receptors on the blood brain barrier luminal face, and then transported into the brain (Prabhakar, 2013). Therefore, incorporation of Tween 80 into the polymeric micelles of poloxamer in the present study was to obtain the most desirable carrier for the chrysin solubilization and delivery system. It was found that chrysin could be loaded into both Pluronic F-68 and Pluronic F-127. The systems obtained after preparation were transparent aqueous dispersions. After lyophilization, the products obtained were still transparent but the state of matter was changed to a semisolid form as a gel-like product. After diluting with water, the semisolid products changed to transparent aqueous systems without any precipitation of chrysin. It was considered that all chrysin could be dissolved in the water. The result was in agreement with the previous results that the practically insoluble curcumin and xanthone could be solubilized by polymeric micelles and transparent aqueous mixtures obtained (Naksuriya, 2015, Khonkarn, 2012).

Two types of solvents, ethanol and acetone, were compared in the preparation of the micelles of two types of poloxamer (P68 and P127). It was found that using ethanol as a solvent for chrysin (assigned as CS) in the preparation of drug loaded micelles yielded micelles with different sizes depending on the polymer type and drug to polymer ratio. The size and PDI as well as % intensity of CS-P68 and CS-P127 are shown in Table 3.4 and Table 3.5, respectively.

Table 3.4 The characteristics of CS-P68 obtained from the use of ethanol as a solvent.

Ratio of chrysin to polymer (w/w)	Size (nm)	PDI	Intensity (%)
0:1	10.40 ± 3.418	0.132	100.0
1:1	17.87 ± 8.378	0.204	98.5
1:2	12.60 ± 4.238	0.156	98.6
1:3	12.59 ± 4.163	0.147	98.6
1:4	12.71 ± 4.102	0.139	100.0
1:5	13.58 ± 4.780	0.192	96.3
1:10	14.38 ± 5.615	0.197	97.0
1:15	15.03 ± 5.262	0.263	95.3

Table 3.5 The characteristics of CS-P127 obtained from the use of ethanol as a solvent.

Ratio of chrysin to polymer (w/w)	Size (nm)	PDI	Intensity (%)
0:1	9.116 ± 2.218	0.166	100.0
1:1	13.82 ± 5.214	0.179	96.8
1:2	11.74 ± 3.222	0.054	100.0
1:3	11.26 ± 2.774	0.195	97.6
1:4	13.38 ± 3.916	0.278	92.1
1:5	13.76 ± 2.916	0.247	79.7
1:10	14.10 ± 3.672	0.315	86.2
1:15	ND	ND	ND

ND = not detectable

It was found that the size of drug entrapped micelles was slightly larger than that of empty micelles for both polymers. The size of CS-P68 was in the range of 12.6-17.8 nm whereas that of CS-P127 was in the range of 11.2-14.1 nm. The PDI was in the range of 0.1-0.2 for CS-P68 and 0.1-0.3 for CS-P127 indicating a good size distribution for both polymers. According to the peak intensity, the mixture at a weight ratio of 1:4

was considered to be the best formulation for CS-P68 whereas that of 1:2 was considered to be the best formulation for CS-P127 because it revealed a peak intensity of 100% as shown in Figure 3.39 and showed zeta potentials in Figure 3.40.

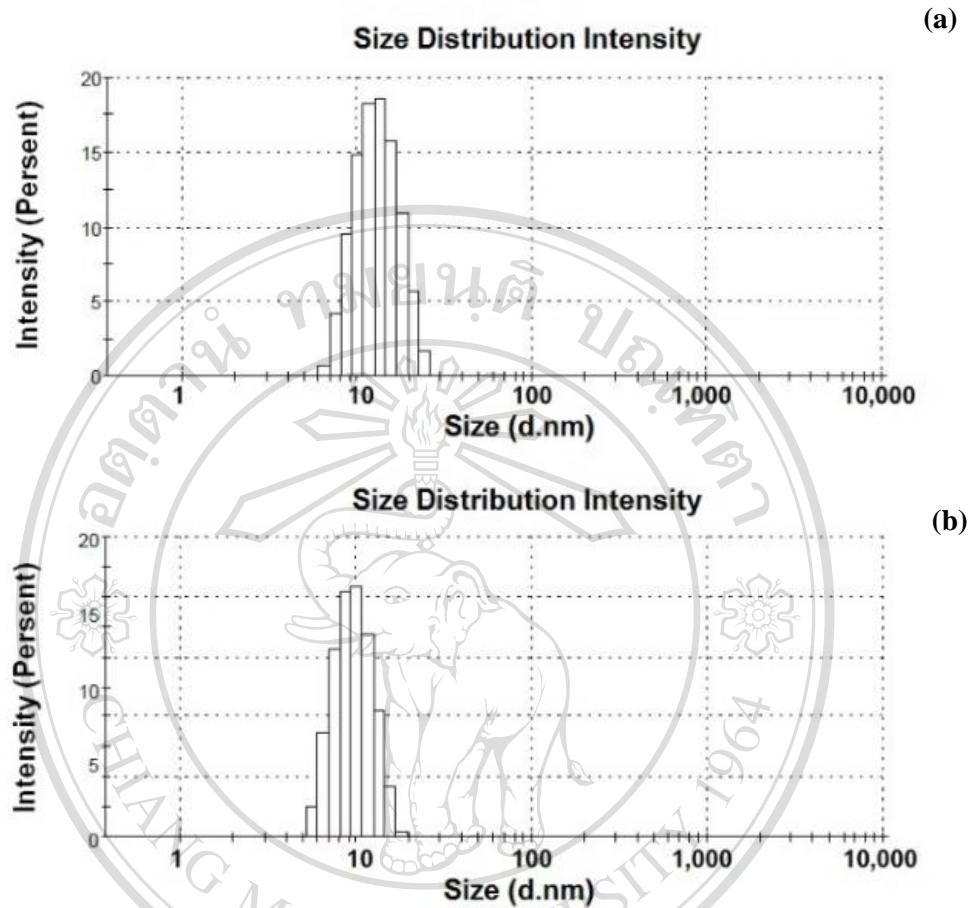


Figure 3.39 The PCS analysis of CS-P68 (a) and CS-P127 (b) at drug to polymer ratios of 1:4 and 1:2, respectively obtained from the use of ethanol as a solvent.

ลิขสิทธิ์มหาวิทยาลัยเชียงใหม่  
Copyright © by Chiang Mai University  
All rights reserved

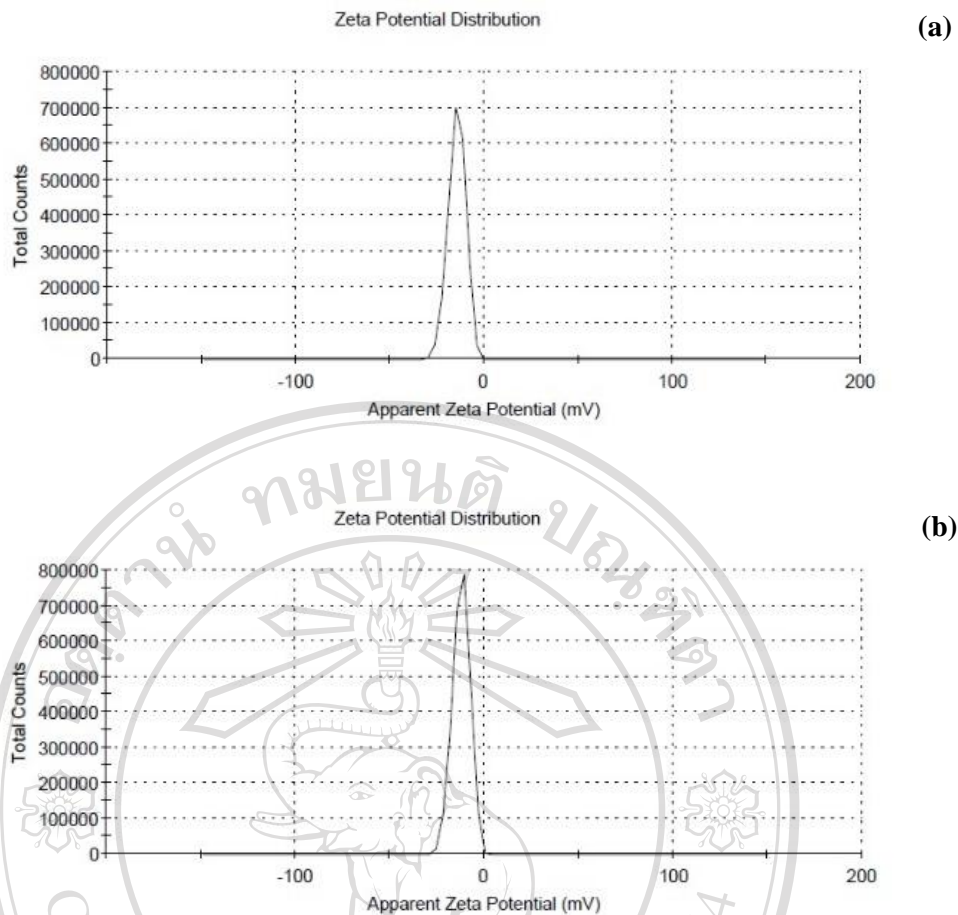


Figure 3.40 The zeta potential analysis of CS-P68 (a) and CS-P127 (b) at drug to polymer ratios of 1:4 and 1:2, respectively obtained from the use of ethanol as a solvent.

The zeta potential of CS-P68 and CS-P127 from the use of ethanol as a solvent at the chrysin to polymer ratios of 1:4 and 1:2 possess zeta potential  $-14.3 \pm 4.66$  and  $-12.1 \pm 4.60$ , respectively. The nanoparticle had high possibility to be aggregated due to zeta potential value of greater than  $\pm 30$  mV is required for a stability (Freitas, 1998)

Using acetone instead of ethanol as a solvent for chrysin to formulate chrysin loaded polymeric micelles of both polymers CS-P68 and CS-P127 could also be obtained. Similarly to those using ethanol as a solvent, it was found that the size of chrysin loaded micelles was slightly larger than that of empty micelles as indicated by Tima (2016). As shown in Table 3.6 and Table 3.7 for CS-P68 and CS-P127, respectively, it was found that the size of CS-P68 and CS-P127 was in the range of 10.5-16.8 nm and 10.1-14.5 nm, respectively

Table 3.6 The characteristics of CS-P68 obtained from the use of acetone as a solvent  
(Mean  $\pm$  SD).

Ratio of chrysin to polymer (w/w)	Size (nm)	PDI	Intensity (%)
0:1	10.25 $\pm$ 2.977	0.076	100.0
1:1	11.47 $\pm$ 3.593	0.112	97.9
1:2	10.70 $\pm$ 3.623	0.181	97.6
1:3	10.56 $\pm$ 3.543	0.126	100.0
1:4	12.07 $\pm$ 4.343	0.259	93.2
1:5	10.83 $\pm$ 3.344	0.215	96.8
1:10	12.46 $\pm$ 5.215	0.193	97.3
1:15	16.82 $\pm$ 6.708	0.217	96.3

Table 3.7 The characteristics of CS-P127 obtained from the use of acetone as a solvent  
(Mean  $\pm$  SD).

Ratio of chrysin to polymer (w/w)	Size (nm)	PDI	Intensity (%)
0:1	9.02 $\pm$ 2.347	0.081	100.0
1:1	10.90 $\pm$ 3.712	0.138	98.8
1:2	11.82 $\pm$ 3.937	0.288	88.6
1:3	10.61 $\pm$ 3.470	0.099	100.0
1:4	8.64 $\pm$ 2.587	0.331	95.7
1:5	14.59 $\pm$ 7.522	0.193	98.7
1:10	11.83 $\pm$ 4.374	0.145	100.0
1:15	11.09 $\pm$ 3.161	0.066	100.0

According to peak intensity, the mixture at a weight ratio of 1:3 was considered to be the best formulation for CS-P68 because this system showed a peak intensity of 100% and showed a single size distribution peak as shown in Figure 3.41 (a). However, three systems of CS-P127 with drug to polymer ratios of 1:3, 1:10, and 1:15 showed a

peak intensity of 100%. Considering the particle size of these systems, it was found that the micelles at a ratio of 1:3 showed the smallest size of  $10.6 \pm 3.4$  nm. The single size distribution peak of this system was obtained as shown in Figure 3.41 (b). It was observed that the size of chrysin loaded micelles prepared using acetone as a solvent for preparation of drug solution was slightly smaller but not significantly different than those using ethanol as a solvent. The PDI of the micelles of both polymers was in the same range as those prepared by using ethanol as a solvent.

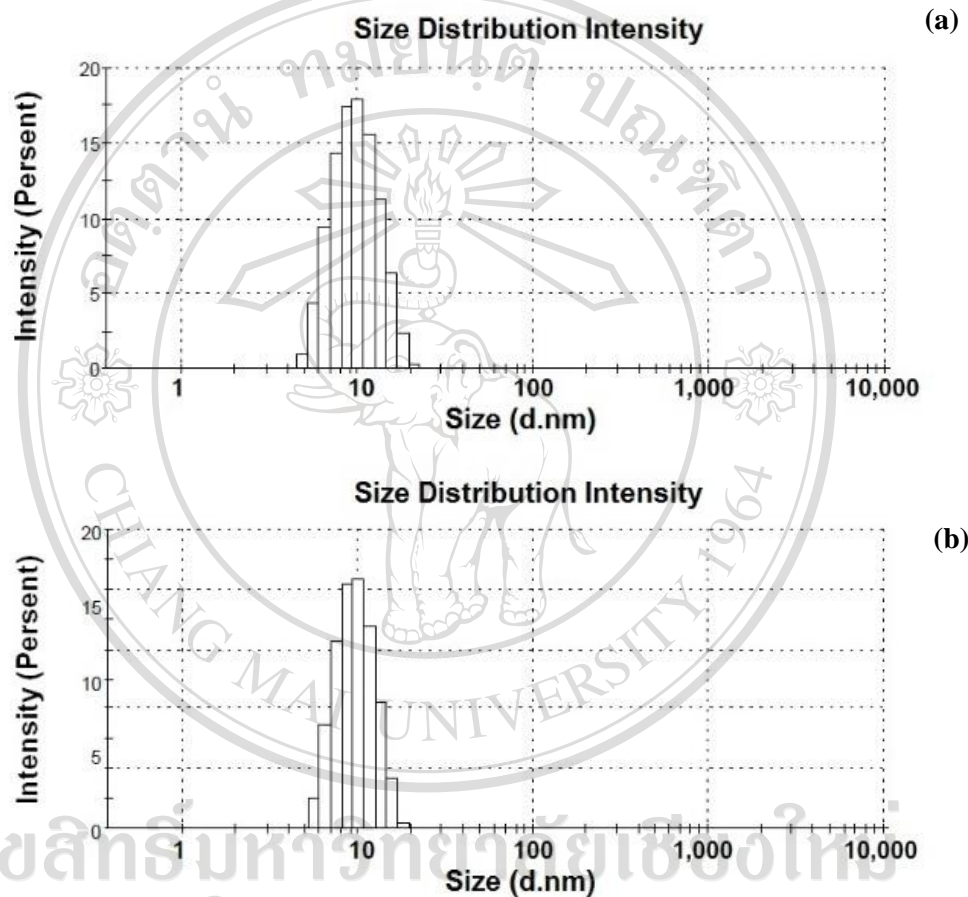


Figure 3.41 The PCS analysis of CS-P68 (a) and CS-P127 (b) at drug to polymer ratio of 1:3 obtained from the use of acetone as a solvent.

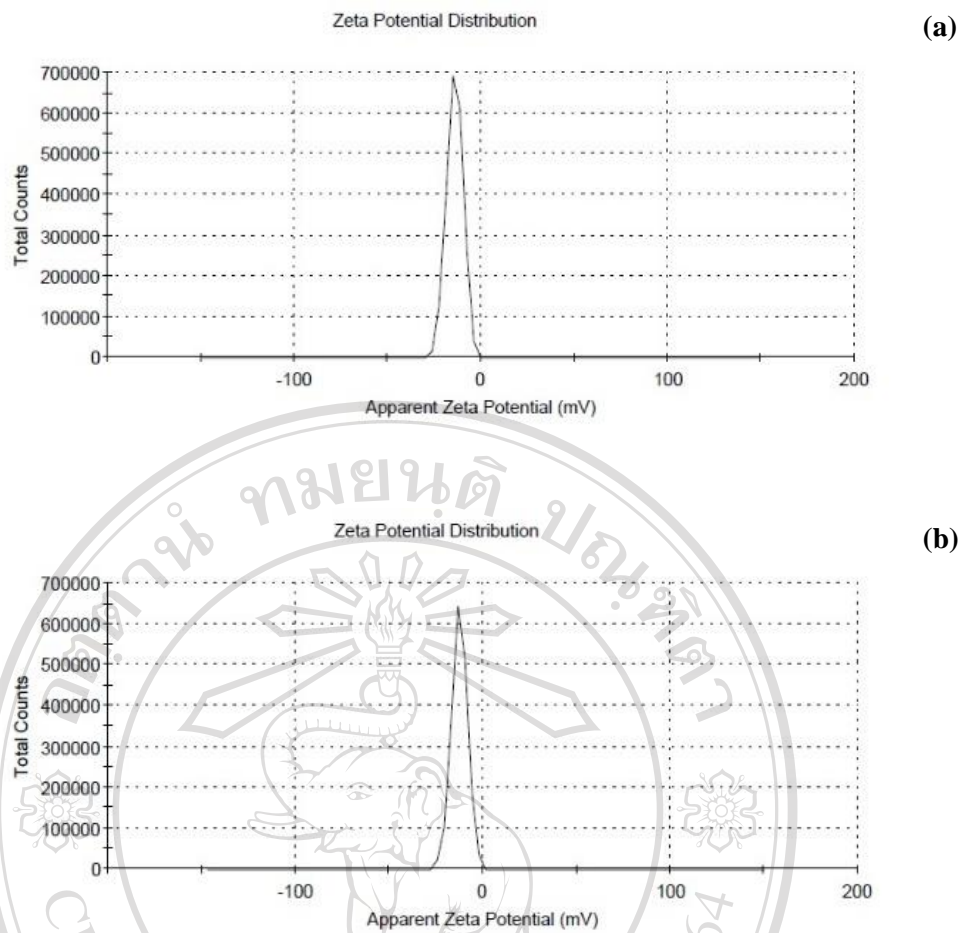


Figure 3.42 The zeta potential of CS-P68 (a) and CS-P127 (b) at drug to polymer ratio of 1:3 obtained from the use of acetone as a solvent.

The zeta potential of CS-P68 and CS-P127 from the use of ethanol as a solvent at the chrysin to polymer ratios of 1:3 possess zeta potential  $-13.9 \pm 4.35$  and  $-12.4 \pm 4.31$ , respectively. It is indicated that both nanoparticles had high possibility to be aggregated as same as prepared by using ethanol due to the zeta potential value was not greater than  $\pm 30$  mV.

The effect of pH on chrysin releasing behavior from CS-P68 and CS-P127 were also examined in 10 mM HEPES buffer. The results were showed in Figure 3.43

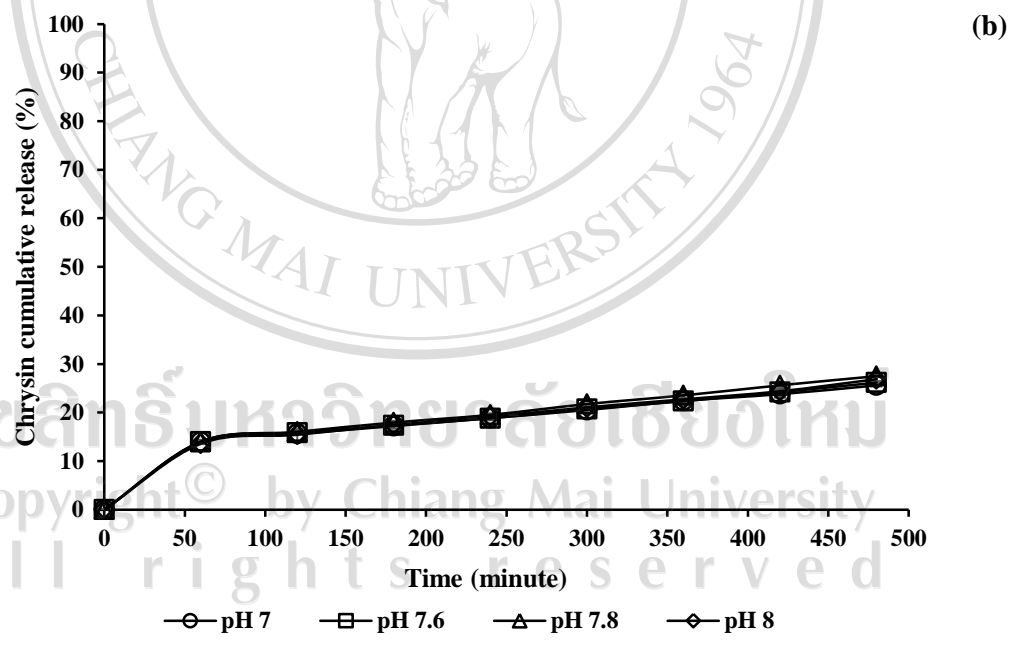
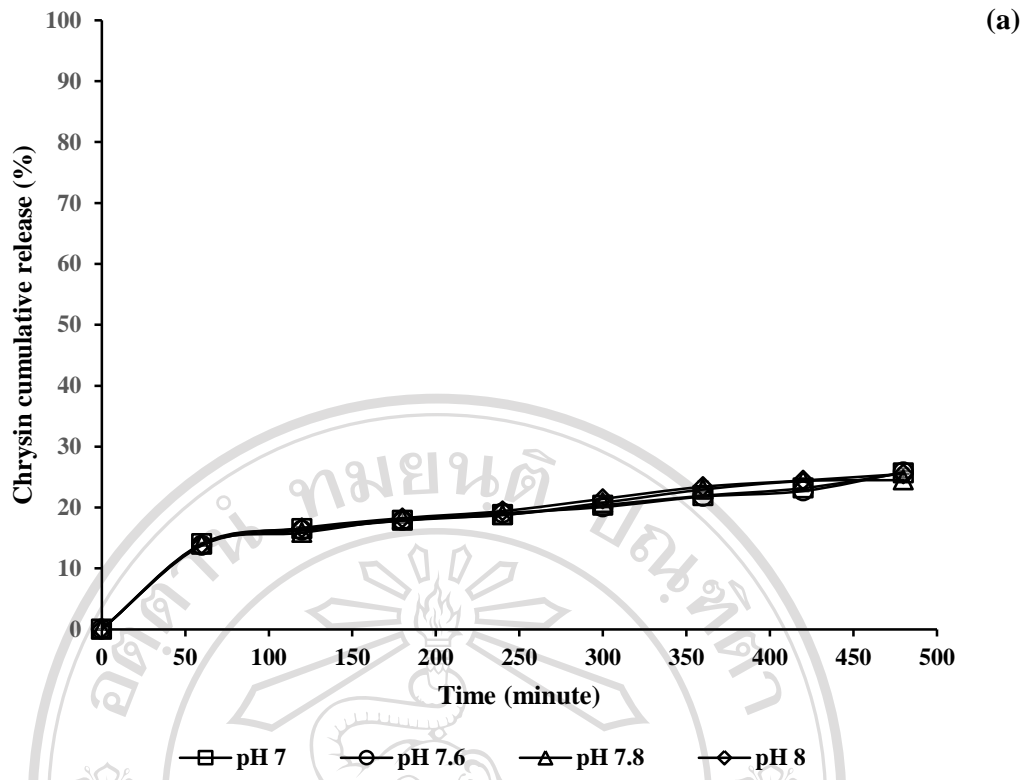


Figure 3.43 The effect of pH on chrysin release behavior from CS-P68 and CS-P127 prepared in proper formulation in 10 mM HEPES buffer.

Figure 3.43 showed *in vitro* chrysin release profiles from polymeric micelles prepared by using ethanol or acetone as solvent. It was indicated that pH of 10 mM HEPES buffer had no effect on drug releasing. The percentage of chrysin in 10 mM HEPES buffer was 15% at first hours and revealed slower releasing compared to releasing of chrysin prepared from HP $\beta$ CD entrapment. The percentage of chrysin from polymeric micelles was nearly 25% at 8 hours. It can be concluded that chrysin releasing rate of CS-P68 and CS-P127 in water was not different from releasing in fish blood circulation.

These results indicate that chrysin can be successfully entrapped in micelles of both types of poloxamers, Pluronic F-68 and Pluronic F-127. The size of CS-P68 and CS-P127 obtained from all studied conditions were in the nanosize range. The results demonstrate that the types of polymers and the ratio of drug to polymer play an important role in the size of the developed drug loaded micelles whereas no significant difference between ethanol and acetone used as a solvent for drug dissolution was seen in the preparation process.

When comparing the developed chrysin loaded polymeric micelles to the intact chrysin added in water, it was found that clear aqueous systems of CS-P68 and CS-P127 were obtained whereas the intact chrysin at the same concentration precipitated in water. This result obviously indicates that water solubility of chrysin was increased dramatically when formed as CS-P68 and CS-P127. As poloxamer is composed of hydrophilic polyethylene oxide (PEO) and lipophilic polypropylene oxide (PPO) blocks, arranged in a PEO<sub>m</sub>PPO<sub>n</sub>PEO<sub>m</sub> structure, where m and n represent the number of monomer in each block (Chiappetta, 2007), they can self-assemble into micelles in aqueous solution forming the hydrophobic PPO core surrounded by the hydrophilic PEO. The increased water solubility of chrysin using these polymeric micelles is considered to be due to the incorporation of chrysin into the hydrophobic portion of the micelles.

Regarding the solvent used, both ethanol and acetone could yield chrysin loaded micelles with a similar nanosize range but ethanol is considered to be a better solvent

than acetone from the view point of environmental and human safety. Therefore, in the investigation of in vivo toxicity, only CS-P68 and CS-P127 with the proper ratio of drug to polymer of 1:4 and 1:2, respectively, and prepared using ethanol as a solvent were used. Chrysin has been reported to suppress an enzyme that converts androgen to estrogen resulting in an increase of testosterone (Jana, 2008). Therefore, it might be useful to know the safe dose or the maximum concentration of CS-P68 and CS-P127 which is considered as safe. In the present study, the embryo of zebra fish was used as a model for testing toxicity of the developed CS-P68 and CS-P127. The toxicity results shown as mortality of zebrafish embryo are in Figure 3.43(a) for CS-P68 and Figure 3.43(b) for CS-P127. From these figures, it was noted that the mortality of the embryos with CS-P68 was higher than that with CS-P127 indicating that CS-P68 had higher toxicity than CS-P127. This effect was obviously seen particularly at the low dose range of 1-100 ng/mL. However, toxicity of both micelles was not significantly different at a concentration of 1000 ng/mL or more. It was found that the toxicity of all samples was seen in a dose dependent manner. A 10 ng/mL dose or less was found to be safe for zebrafish embryos as less than 10% mortality was observed whereas doses of 100-1,000 ng/mL could be classified as a mild toxic dose as 10% to less than 30% mortality was observed. Higher than 1,000 ng/mL could be classified as moderate to severe toxicity to zebrafish embryos as 30-100% mortality was observed. The results also showed that the toxic effect of CS-P68 and CS-P127 was not time dependent. After incubating zebrafish eggs in the fixed drug dose systems but at different incubation times of 24, 48, and 72 h, the mortality of the fish was not significantly different at each dose as indicated in

F i g u r e 3 . 4 4 .

ลิขสิทธิ์มหาวิทยาลัยเชียงใหม่  
Copyright© by Chiang Mai University  
All rights reserved

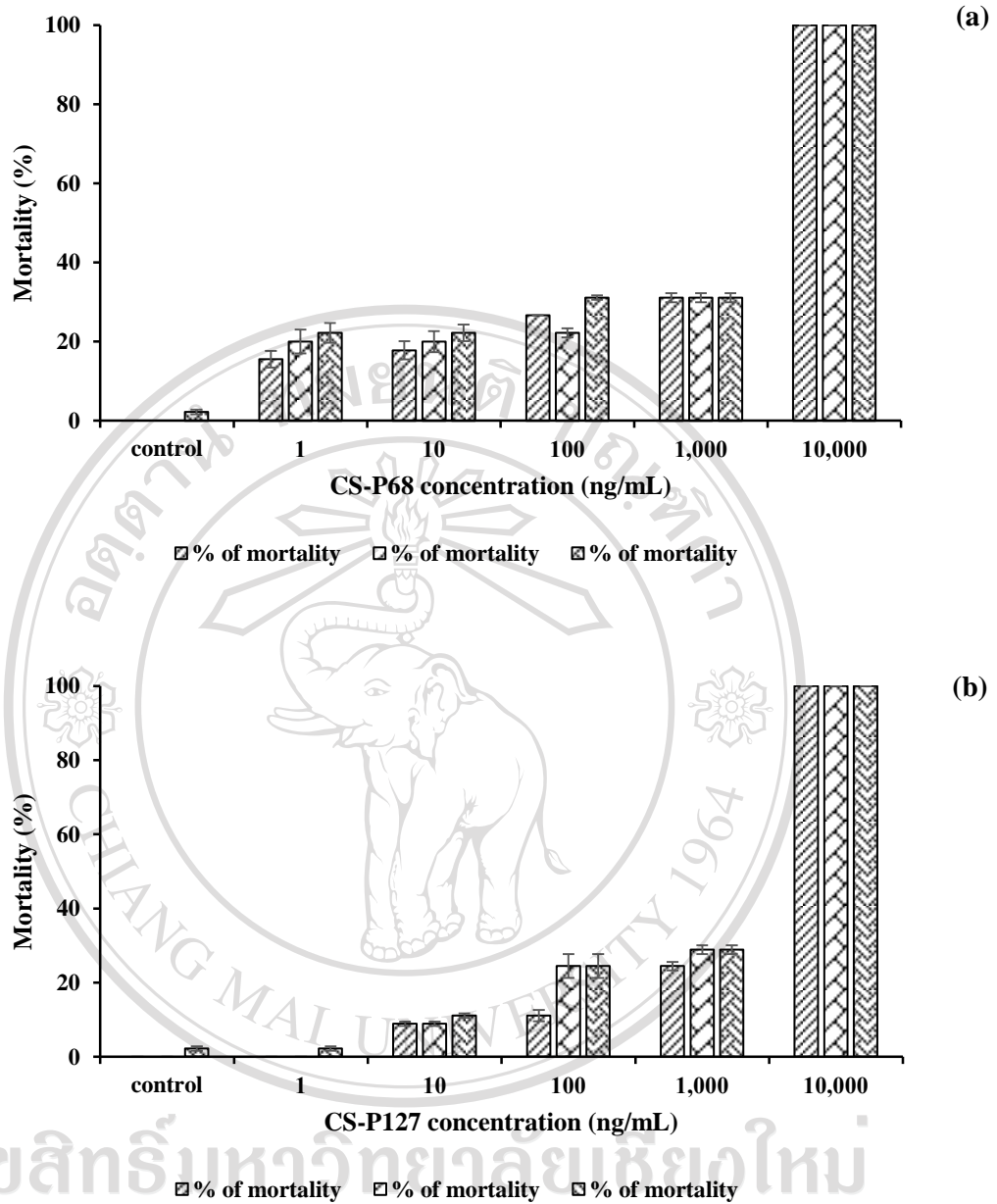


Figure 3.44 The mortality of zebrafish eggs at 24 h, 48 h, and 72 h exposure to CS-P68 (a) and CS-P127 (b)

The results revealed that no zebrafish embryos were found after 24 hours exposure to 10,000 ng/mL whereas more than 70% of the embryos developed normally (same as control) after exposure to 1-100 ng/mL. However, at a concentration of 1,000

ng/mL, some embryos (about  $27 \pm 1\%$ ) were dead after 24 hours of exposure, the remaining embryos could develop but some showed delayed development. This effect could be seen clearly as shown in Figure 3.44. After 72 h, all embryos in the control group could hatch normally whereas only approx.  $55 \pm 5\%$  of the eggs exposed to CS-P68 and CS-P127 (1,000 ng/mL) showed normal development like in the control group but the remaining embryos were still at an early stage. They were not dead but showed slow development as seen in Figure 3.45(c). It was considered that polymer might be associated with the toxicity of CS-P68 and CS-P127. In CS-P68, the drug to polymer ratio was 1:4 whereas in CS-P127 it was 1:2. The amount of polymer in CS-P68 was 2 times higher than that in CS-P127. Therefore, high mortality particularly at low drug concentrations caused by CS-P68 was considered to be due to high concentration of polymer used in CS-P68.

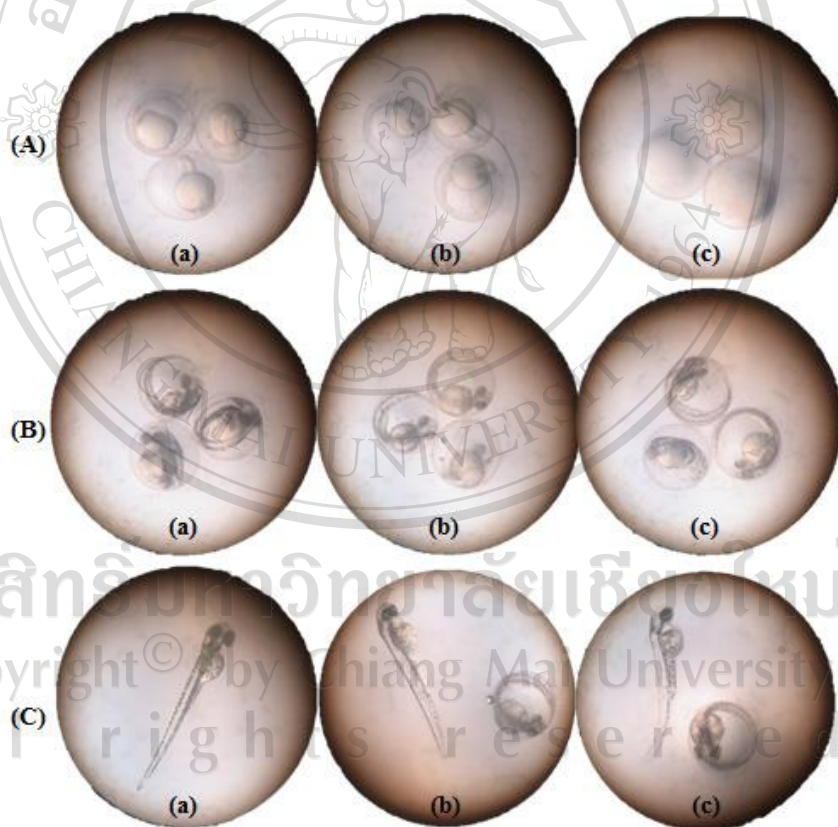


Figure 3.45 The morphology of surviving zebrafish embryos at 24 hours (A), 48 hours (B), and 72 hours (C) exposure to water (a), CS-P68 at drug concentration of 1,000 ng/mL (b), and CS-P127 at drug concentration of 1,000 ng/mL (c).

### 3. PLGA entrapment

The particle size, PDI, zeta potential, and intensity are the most important of physicochemical properties for drug delivery systems. The mean particle diameter and zeta potential of the polymeric nanoparticles produced was measured and indicate in the Table 3.8. Molecular weight (MW) and concentration of PLGA used are key factors that can affect the final size of the nanoparticles (Song, 2008).

Table 3.8 Mean particle size, zeta potential, PDI, intensity, and encapsulation efficiency of chrysin loaded PLGA (Mean  $\pm$  SD).

Ratio of Chrysin : PLGA	Particle size (nm)	Zeta potential (mV)	PDI	Intensity (%)	% EE
1:0	9.6 $\pm$ 3.28	-4.33 $\pm$ 7.05	0.100	100.0	-
1:1	111.5 $\pm$ 37.14	-4.95 $\pm$ 12.70	0.673	69.4	49.13
1:2.5	163.8 $\pm$ 52.92	-1.46 $\pm$ 6.91	0.286	100.0	51.56
1:5	205.0 $\pm$ 59.69	-1.40 $\pm$ 6.45	0.124	100.0	56.99
1:7.5	276.9 $\pm$ 85.13	-0.96 $\pm$ 4.65	0.105	100.0	54.72
1:10	368.4 $\pm$ 150.80	-1.04 $\pm$ 4.86	0.152	100.0	40.53
1:12.5	476.0 $\pm$ 122.40	4.13 $\pm$ 3.96	0.085	100.0	ND

ND = not detectable

These results indicated that chrysin was successfully entrapped in micelles by PLGA in cooperated with tween 80. The MW of the PLGA (50:50, PURASORB PDLG) used was low resulted low viscosity of the internal phase, leading to enhance net shear stress, and generate the moderate nanoparticle size. The narrow PDI values indicated that the chrysin loaded nanoparticles obtained by the hot air oven drying method were homogeneous with high intensity. The percentage of entrapment efficiency was performed by indirect method. It was found in that the ratio of chrysin: PLGA, 1:5 had the greatest percentage of entrapment efficiency at 56.99 with high

intensity and low PDI value. The size range of nanoparticles were compared as indicated in Figure 3.46.

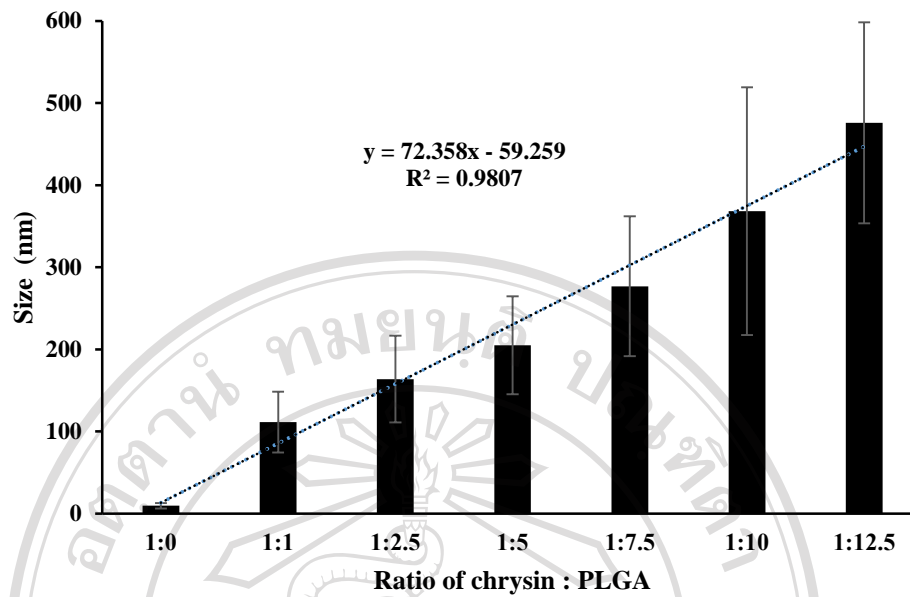


Figure 3.46 The effect of chrysin:PLGA ratio on mean diameter

All sizes of chrysin loaded PLGAs were exhibited a diameter in the nano-size range. The results demonstrate that the ratio of drug to polymer play an important role in the size of the developed drug loaded micelles. This phenomenon was observed by the other research such as Song (2008), Mainardes (2005), and Kwon (2001). However, it maybe also resulted of aggregation of free PLGA or increasing of viscosity of the organic phase. Moreover, the increasing of PLGA maybe lead to insufficiency of surfactant to cover the nanoparticle surfaces. Thus, the coalescence of nanoparticles during organic phase evaporation was happened and affected to aggregation of nanoparticles.

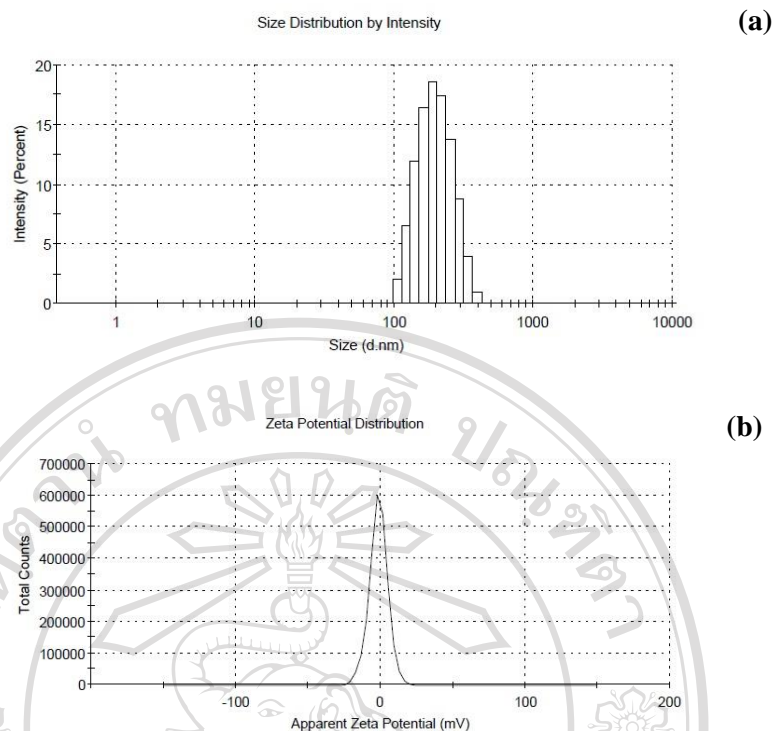


Figure 3.47 The PCS analysis of proper chrysin loaded PLGA

The unimodal histogram of proper chrysin-PLGA ratio on the mean diameter was showed in Figure 3.47(a). The nanosize range of  $205.0 \pm 59.69$  was selected for further study due to larger nanosize cannot be filtrated in spleen while the smaller leaved in the blood vessels (Tabata, 1990; Stolnik, 1995). Moreover, the ratio 1:5 (chrysin:PLGA) revealed the highest entrapment efficiency (56.99 %). However, the zeta potential of chrysin loaded PLGA was closely to zero as indicated in Figure 3.47(b). It can be confirmed that each nanoparticle was not stable. However, the releasing of chrysin was also important. The results of chrysin releasing in various pH buffer were indicated in Figure 3.48.

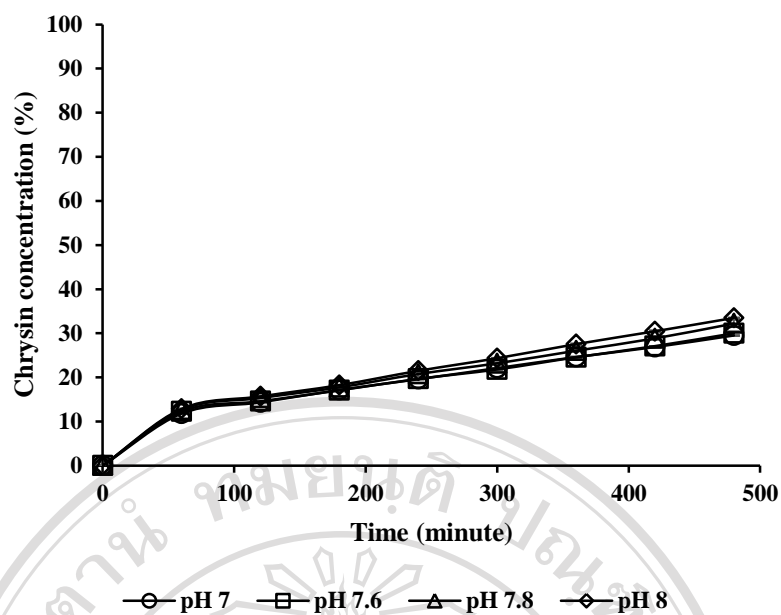


Figure 3.48 The effect of pH on chrysin release behavior from chrysin loaded PLGA in 10 mM HEPES buffer

Figure 3.48 showed *in vitro* chrysin release profiles of chrysin loaded PLGA. It was indicated that 10 mM HEPES buffer, pH 7.0, 7.6, 7.8 and 8.0 had no effect on drug releasing. The percentage of released chrysin in 10 mM HEPES buffer was 12% at first hour and has slow releasing rate compared to the releasing of chrysin from chrysin loaded HP $\beta$ CD. The percentage of chrysin from polymeric micelles was closely 30-35% at 8 hours. It can be concluded that chrysin releasing rate in water was not different from in fish blood circulation.

Mortality of zebrafish eggs at 24 h, 48 h, and 72 h exposure to chrysin loaded PLGA was investigated. The result of mortality was revealed in Figure 3.49

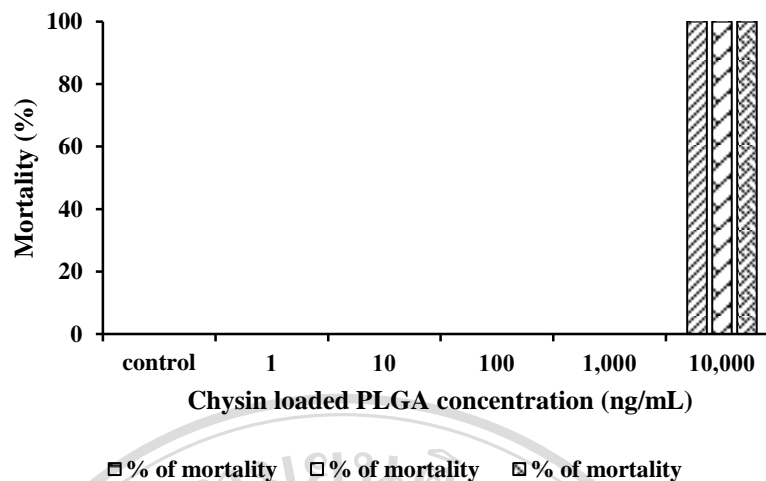


Figure 3.49 The mortality of zebrafish eggs at 24 h, 48 h, and 72 h exposure to chrysin loaded PLGA

The 10-1,000 ng/mL dose were found to be safe for zebrafish embryos as no mortality was observed whereas doses of 10,000 ng/mL could be classified as a highly toxic dose. The results also showed that the toxic effect of chrysin loaded PLGA was not time dependent. After incubating zebrafish eggs in the fixed drug dose systems but at different incubation times of 24, 48, and 72 h, the mortality of the fish was not significantly different at each dose. The results revealed that no zebrafish embryos were found after 24 hours exposure to 10,000 ng/mL whereas 100% of the embryos were hatchable after exposure to 1-1,000 ng/mL. However, at a concentration of 10, 100, and 1,000 ng/mL, some embryos (about 5, 55,  $62 \pm 0.5\%$ , respectively) showed delayed development after 24 hours of exposure (Figure 3.50).

Copyright © by Chiang Mai University  
All rights reserved

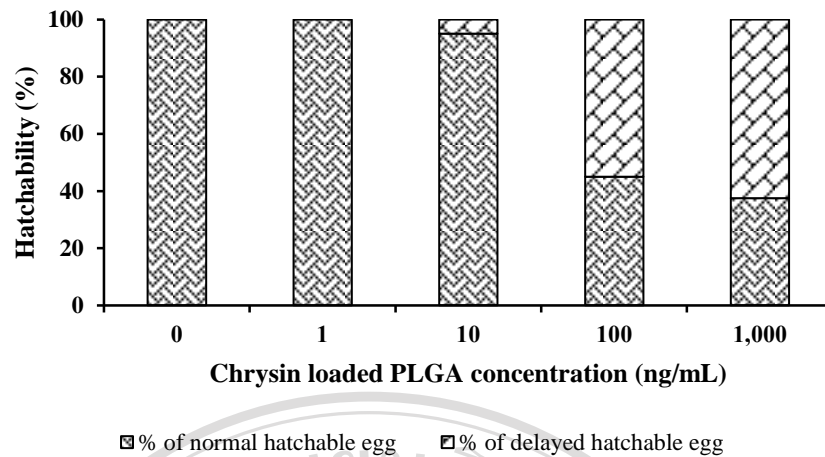


Figure 3.50 The effect of chrysin loaded PLGA on hatchability of zebrafish eggs

The remaining embryos could develop normally. After 72 h, all embryos in the control group could be hatched normally. It was considered that increasing of polymer concentration might be associated with the toxicity.

#### 4. Bilosome entrapment

To formulate the bilosome, different types of surfactants were used in formulation resulted in different types of non-ionic vesicles in terms of their sizes, percentage of entrapment efficiency and stability (Uchegbu, 1999). Bilosome was immerse to drug delivery system due to its ability in hydrophobic entrapment. Chrysin maybe entrapped into the hydrophobic part by incorporate into surfactants, cholesterol, and bile acid at the proper ratio.

Table 3.9 The effect of surfactants on bilosome formation and their properties  
(Mean  $\pm$  SD).

Surfactant	formula	Major Size (nm)	PDI	% of intensity
Span 60	F1	678.9 $\pm$ 85.08	0.494	100.0
	F2	3098 $\pm$ 1214.00	1.000	77.8
	F3	1179 $\pm$ 484.70	0.609	61.6
Span 80	F4	164.0 $\pm$ 72.10	0.396	81.0
	F5	184.7 $\pm$ 80.12	0.318	88.4
	F6	157.2 $\pm$ 66.00	0.714	60.6
Tween 80	F7	2291 $\pm$ 498.70	0.277	55.7
	F8	3327 $\pm$ 244.20	0.249	87.5
	F9	3.129 $\pm$ 0.00	0.098	100.0
Tween 20	F10	892.4 $\pm$ 65.17	0.505	100.0
	F11	4693 $\pm$ 698.90	0.004	100.0
	F12	5000 $\pm$ 620.10	0.280	100.0

Chrysin loaded bilosome were formed by the presence of non-ionic surfactants in organic phase. The effect of these non-ionic surfactants were varied in molar concentration as recommended of Uchegbu (1998), as well as when added cholesterol (Manosroi, 2008). In this study, Span 80 enable form chrysin loaded bilosome in nanosize range with highest percentage of entrapment efficiency (Table 3.9). It can be

considered that polyoxyethylene head group of span 80 maybe the cause for enhancing the entrapment efficiency due to its ability to form hydrogen bonds with the phenol groups of chrysin molecules. This phenomenon was observed for Morin (3,5,7,2',4'-pentahydroxyflavone) (Waddad, 2013) which has physico-chemical property similar to chrysin (5,7-Dihydroxyflavone). The lower HLB value of Span 80 maybe employed higher entrapment efficiency (Bayindir, 2010). The chrysin loaded bilosome showed the entrapment efficiency in the range of  $93.64 \pm 2.60\%$  with nanosize range of  $164.0 \pm 72.10$  to  $184.7 \pm 80.12$  nm. The unsaturated double bond in Span 80 allow rotation of the alkyl group that maybe contributed reducing its ability to entrap higher amount of chrysin (Lo, 2010; Uchegbu, 1998). The histogram of the proper formulate chrysin loaded bilosome was demonstrated in Figure 3.51.

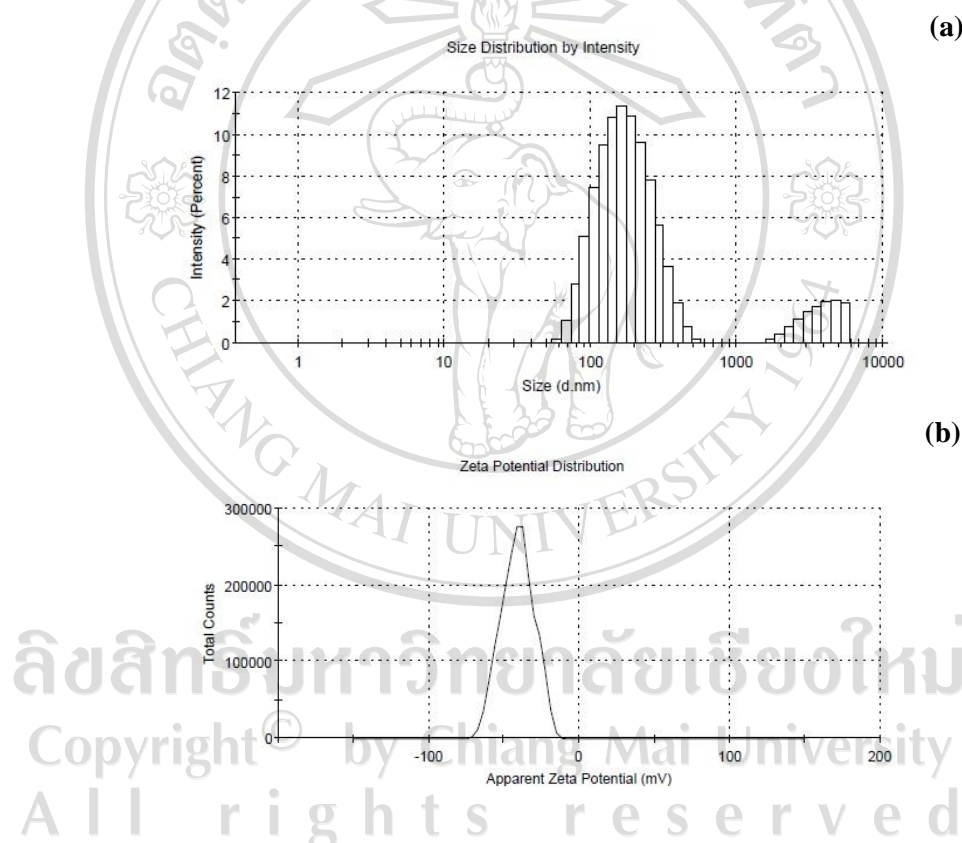


Figure 3.51 The PCS analysis of size and zeta potential of chrysin loaded bilosome.

The nanosize range of  $184.7 \pm 80.12$  was obtained from using Span 80 as surfactant in the F5 formula which composed with 4 moles of surfactant, 4 moles of cholesterol and 0.2 mole of bile acid. The zeta potential was greater than  $-40$  mV that

contribute the high stable bilosome. It can be confirmed that each nanoparticle could be not aggregated. However, the releasing of chrysin from bilosome in various pH was also investigated. The results were indicated in Figure 3.52.

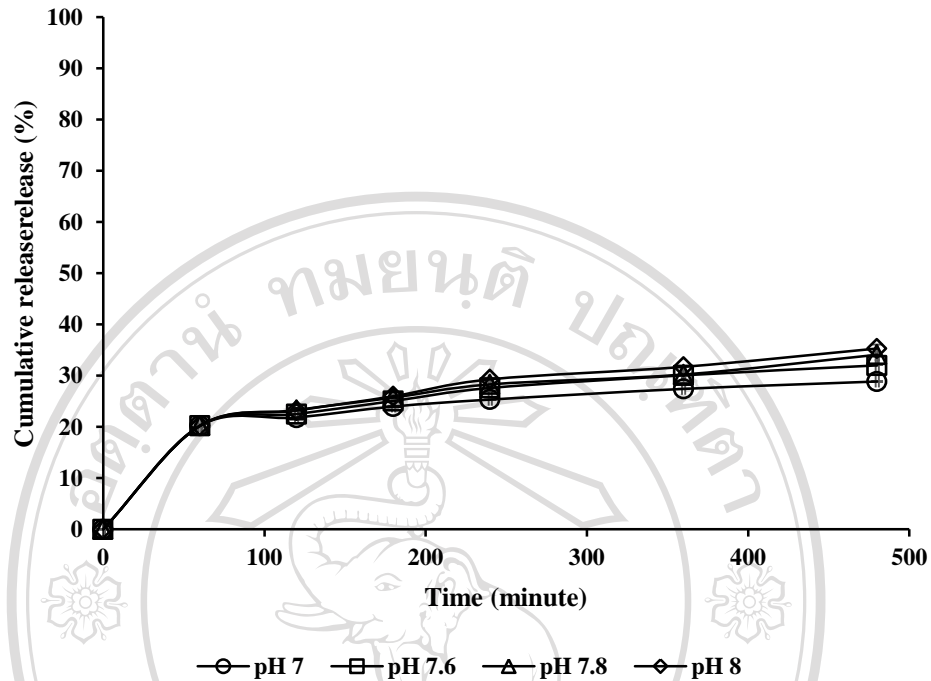


Figure 3.52 The effect of pH on chrysin release behavior from chrysin loaded bilosome in 10 mM HEPES buffer

Figure 3.52 showed *in vitro* chrysin release profiles of bilosome. It was indicated that 10 mM HEPES buffer, pH 7.0, 7.6, 7.8 and 8.0 had no effect on drug releasing. The percentage of released chrysin in 10 mM HEPES buffer was 20% at first hour and revealed slower releasing rate compared to the releasing of chrysin from chrysin loaded HP $\beta$ CD. The percentage of chrysin from bilosome was closely 25-35% at 8 hours. It can be concluded that chrysin releasing rate of chrysin loaded PLGA in water was not different from in fish blood circulation.

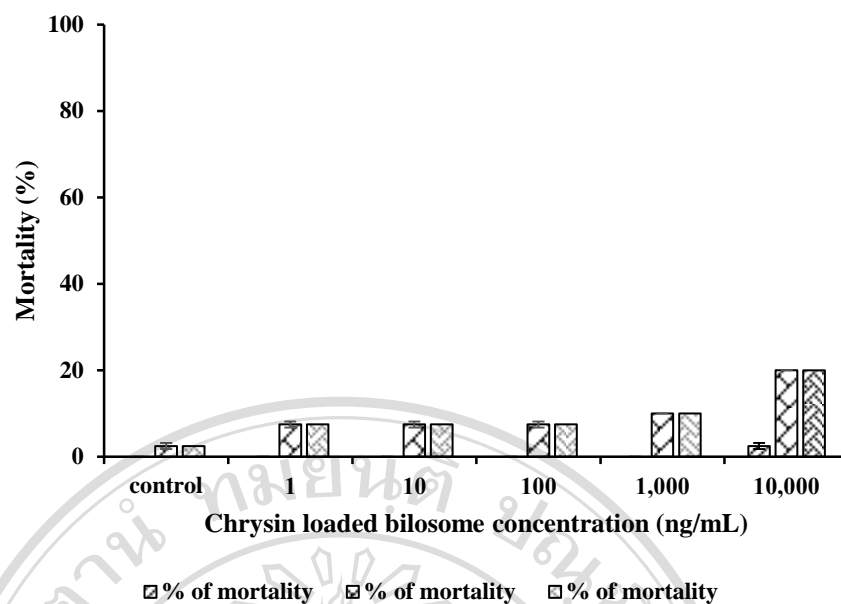


Figure 3.53 The mortality of zebrafish eggs at 24 h, 48 h, and 72 h. exposure to chrysin loaded bilosome

The 10-1,000 ng/mL dose were found to be safe for zebrafish embryos as less than 10% mortality was observed whereas doses of 10,000 ng/mL could be classified as a mild toxic dose as 20% mortality was observed. The results showed that the toxic effect of chrysin loaded bilosome was time dependent. After incubating zebrafish eggs in the fixed drug dose systems but at different incubation times of 24, 48, and 72 h, the mortality of the fish was significantly different at each dose on first day. The results also revealed that nearly 90% of the embryos developed normally (same as control) after exposure to 1-10,000 ng/mL. After 72 h, all embryos could be hatched with some abnormal development. A few depigmented embryos were showed (in Figure 3.54) after exposure to 1-10,000 ng/mL. It was considered that the abnormality might be associated with the toxicity of Span 80 (Ingram, 1978) and bile acid (Attili, 1986). However, the chrysin loaded bilosome was considered to be less toxicity systems to delivery chrysin into fish target cells.

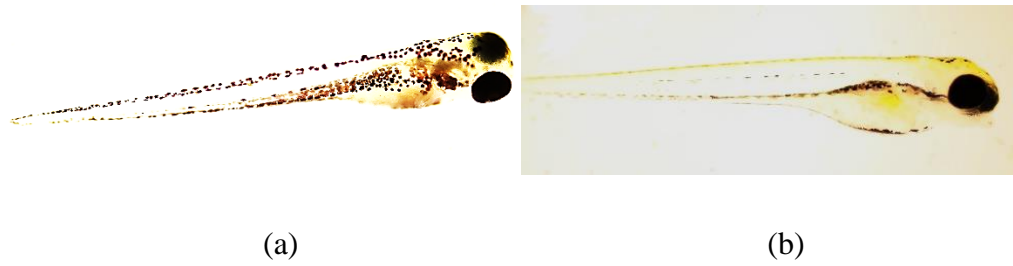
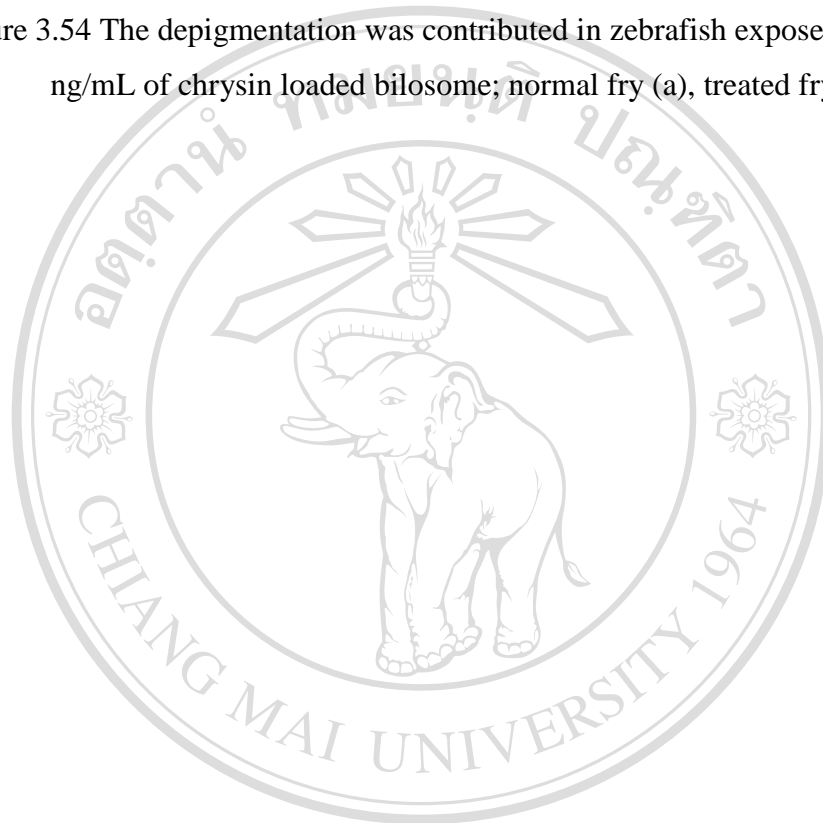


Figure 3.54 The depigmentation was contributed in zebrafish exposed to 1-10,000 ng/mL of chrysin loaded bilosome; normal fry (a), treated fry (b).



ลิขสิทธิ์มหาวิทยาลัยเชียงใหม่  
Copyright© by Chiang Mai University  
All rights reserved

#### **Part IV Zebrafish treatment**

The data from all experimental were compared and indicated that chrysin loaded HP $\beta$ CD had high effectiveness for zebrafish masculinization due to their physicochemical properties and cost effectiveness. The 6 adult zebrafish were treated as indicated in Table 3.10.

Table 3.10 The standard length, body height and weight of experimental zebrafish (Mean  $\pm$  SD)

<b>Group</b>	<b>Standard Length (mm)</b>	<b>Body height (mm)</b>	<b>Weight (g)</b>
Control male	2.83 $\pm$ 0.29	0.50 $\pm$ 0	0.30 $\pm$ 0.07
Control female	2.73 $\pm$ 0.06	0.70 $\pm$ 0	0.37 $\pm$ 0.02
Vehicle treatment	2.90 $\pm$ 0.17	0.80 $\pm$ 0	0.41 $\pm$ 0.09
10 ng/mL treatment	2.87 $\pm$ 0.23	0.50 $\pm$ 0	0.26 $\pm$ 0.04
100 ng/mL treatment	2.90 $\pm$ 0.10	0.53 $\pm$ 0	0.31 $\pm$ 0.10

The standard length of zebrafish were not different significantly both in control group (n=6) and treated group (n=6) after exposure to chrysin loaded HP $\beta$ CD for 60 days. Interestingly, the body height and weight of 10 ng/mL treatment and 100 ng/mL treatment trend to closely control male group. Furthermore, the zebrafish group of vehicle and control female seem to be not different in size range. The other characteristics were revealed in Figure 3.55.

ลิขสิทธิ์มหาวิทยาลัยเชียงใหม่  
Copyright© by Chiang Mai University  
All rights reserved

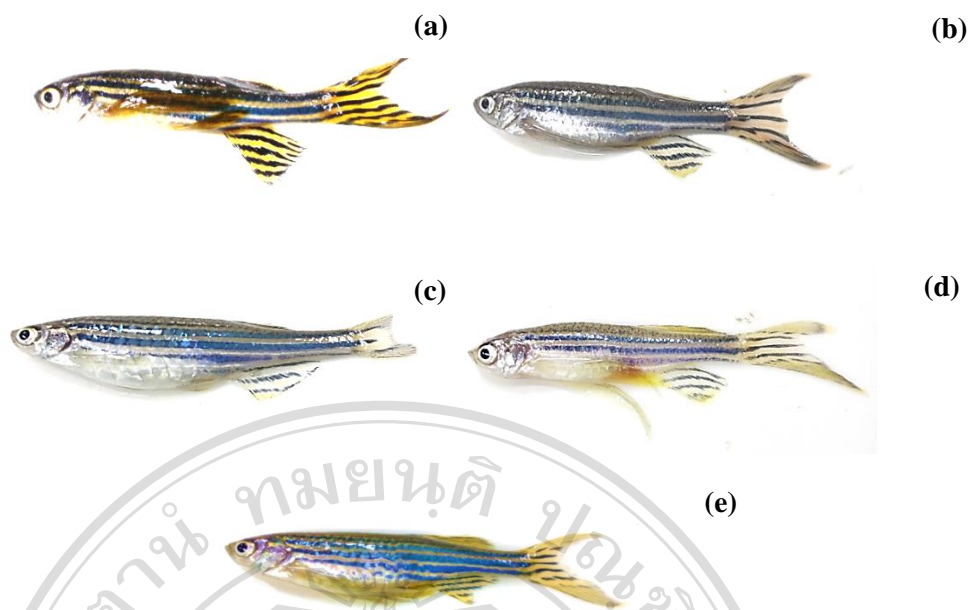


Figure 3.55 The characteristic of (a) male, (b) female, (c) vehicle control female, (d) 10 ng/mL of nanochrysin treated female and (e) 100 ng/mL of chrysin-loaded HP $\beta$ CD treated female adult zebrafish.

The male and female zebrafish has different body shape and coloring (Figure 3.55). The body shape of adult male zebrafish is slender with strong yellow color fin compared to the female. Female can also be notable from males by a silvery-blue line on the lateral side of the body. To investigate the effect of chrysin-loaded HP $\beta$ CD in gonad of zebrafish. Fish was euthanized and examined after staining with H&E solution. The morphology of gonad of control and treated group were examined under microscopy. The results were revealed as Figure 3.56-3.58.

Copyright© by Chiang Mai University  
All rights reserved

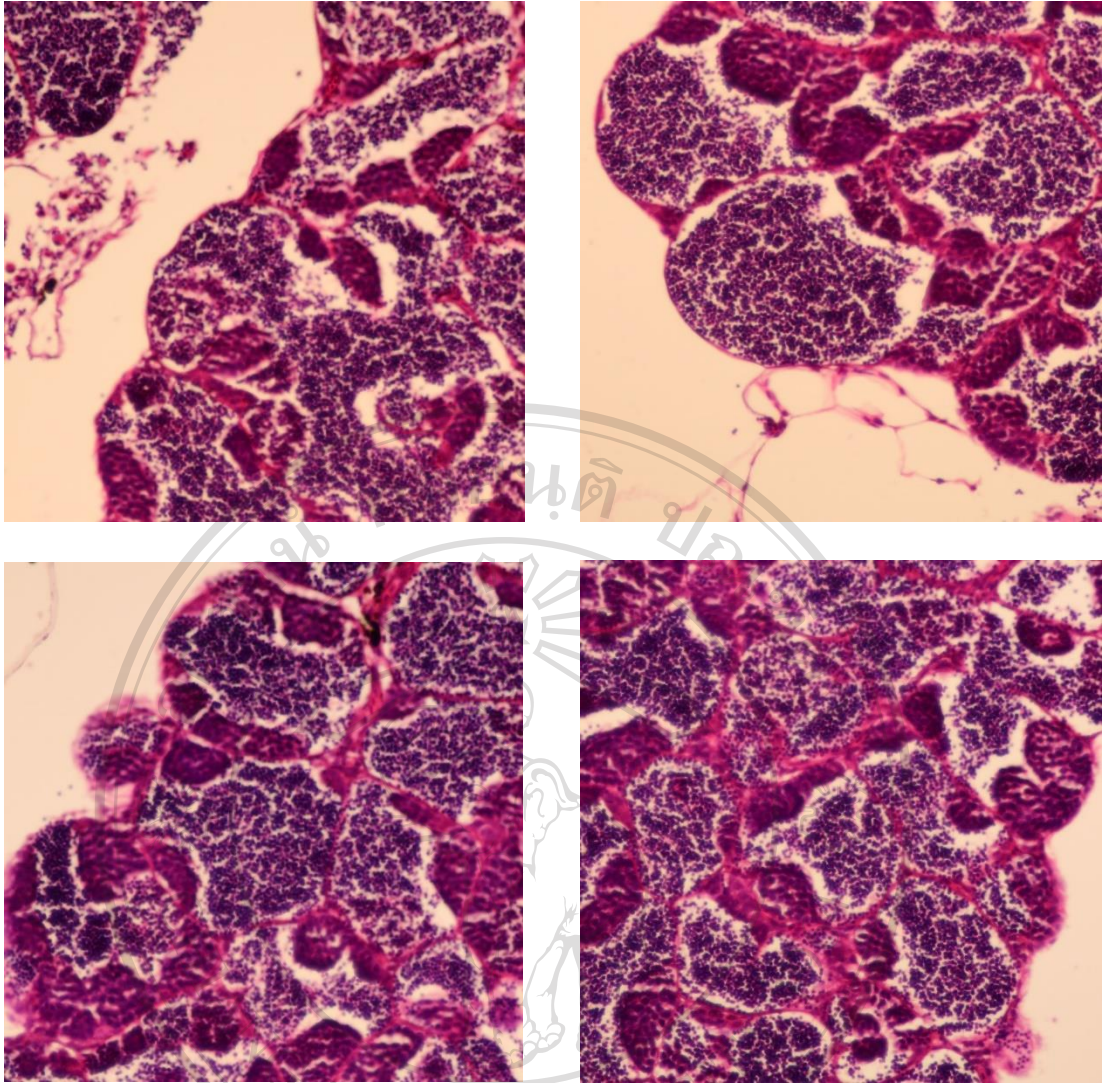


Figure 3.56 The histological observations of male gonads (400X, H&E staining)

ลิขสิทธิ์มหาวิทยาลัยเชียงใหม่  
Copyright© by Chiang Mai University  
All rights reserved

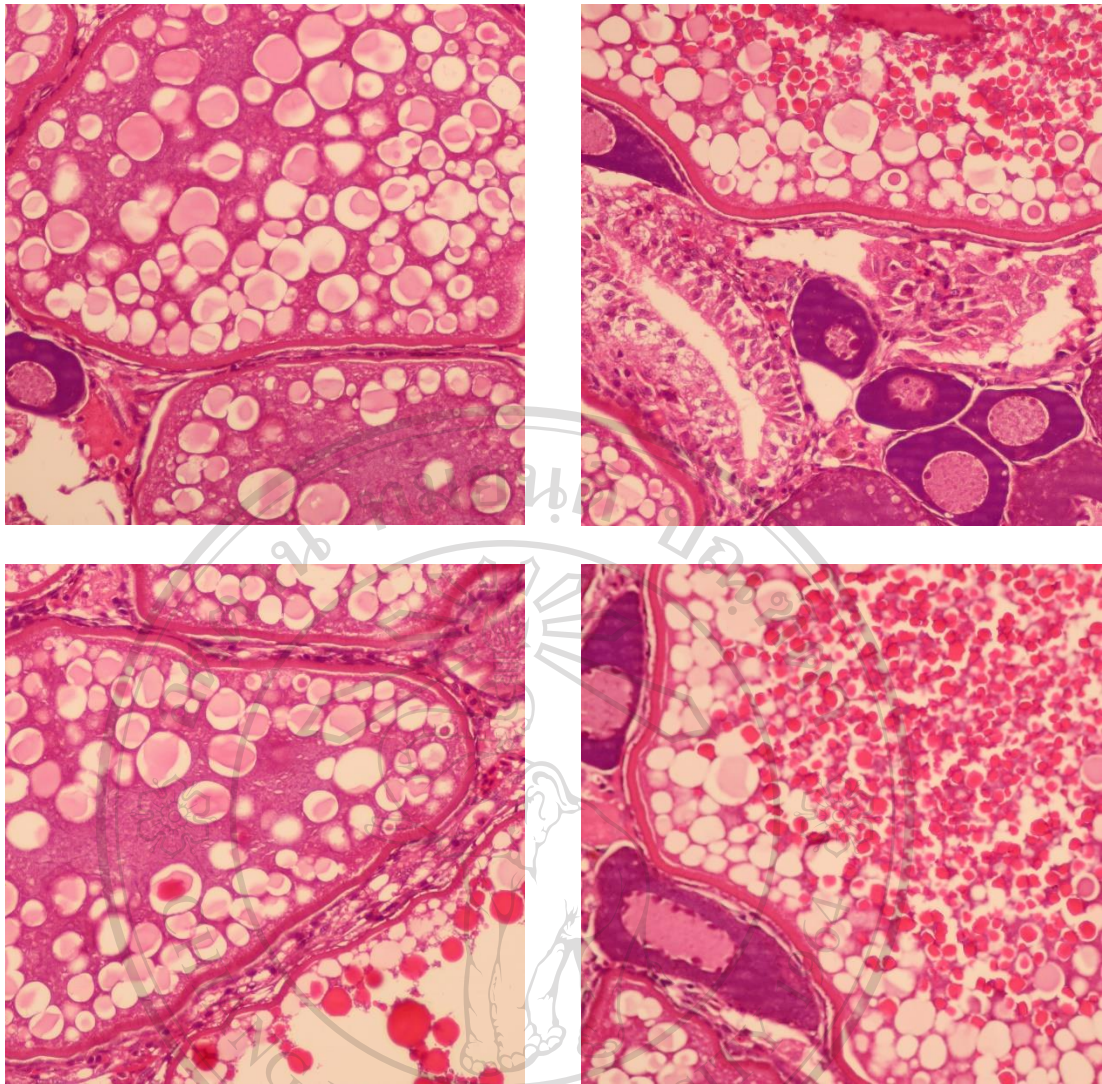


Figure 3.57 The histological observations of female gonads (400X, H&E staining)

ลิขสิทธิ์มหาวิทยาลัยเชียงใหม่  
Copyright© by Chiang Mai University  
All rights reserved

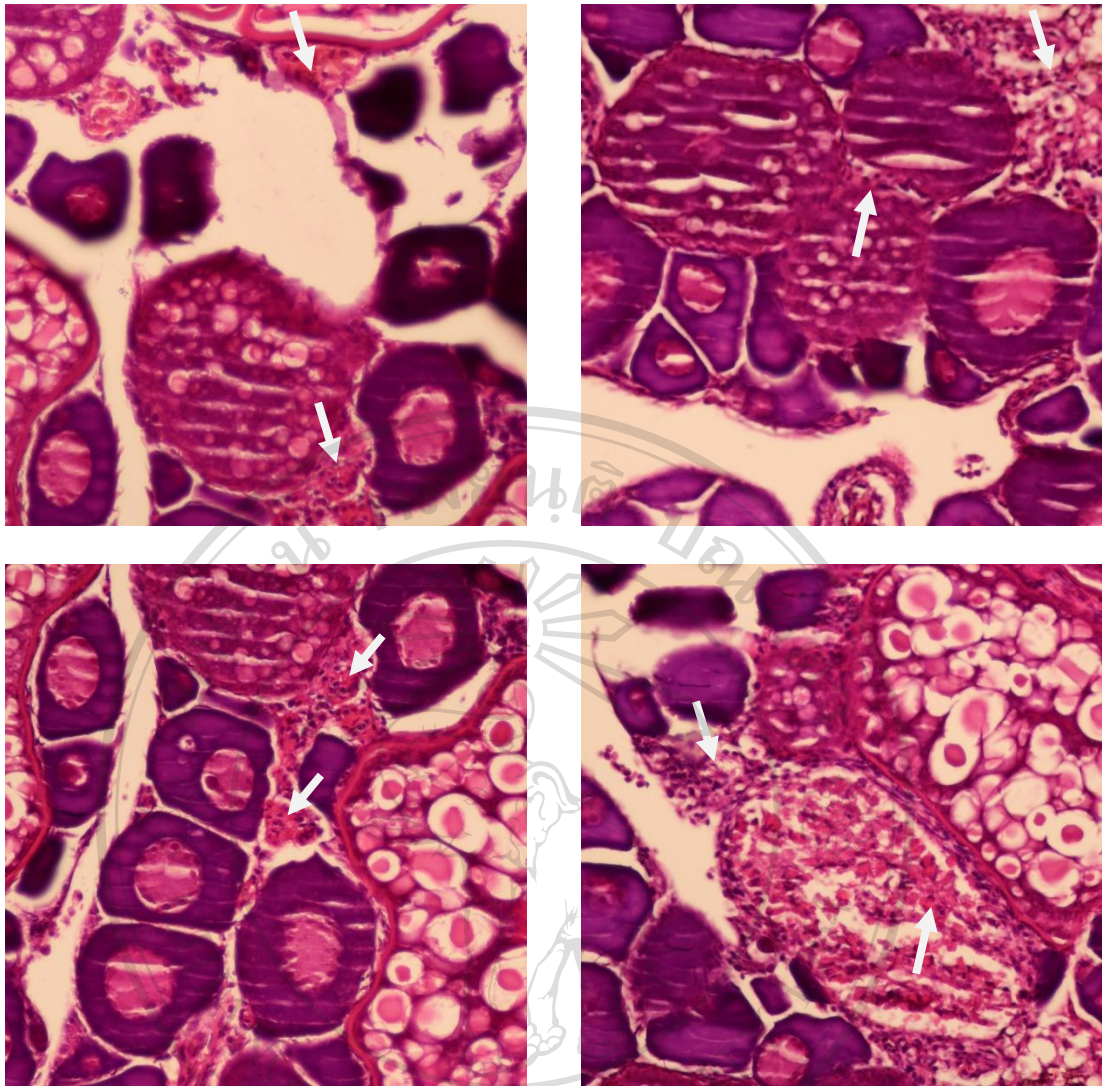


Figure 3.58 Histological observations of chrysin-loaded HP $\beta$ CD treated female gonads (400X, H&E staining)

The histology of male and female was typical ovaries and testes, in which the former were mainly consisted of sperms as indicated in Figure 3.56 and the oocytes from perinucleola to vitellogenic phase as represented in figure 3.57. Interestingly, some fish subjected to the chrysin-loaded HP $\beta$ CD treatments displayed spermatogonia-like gonads as showed in figure 3.58 (white arrow). The same effect has been reported for the synthetic aromatase inhibitor (fadrozole and 17 $\alpha$ -methyltestosterone) treatment in zebrafish during the critical period of gonadal differentiation (Takatsu, 2013; Fenske, 2004). As the results, it can be suggested that decreasing of estrogen influenced to triggering the retraction of ovary and inducing spermatogonia-like gonads formation

and supported the finding of Dranow (2013) that found adult female zebrafish could be masculinized to fully functional males.

Interestingly, this is the first report that demonstrated natural aromatase inhibitor, chrysin, solubilized by using HP $\beta$ CD can induce adult female-to-male sex change in adult zebrafish.



ลิขสิทธิ์มหาวิทยาลัยเชียงใหม่  
Copyright© by Chiang Mai University  
All rights reserved